KTH Engineering Sciences

Masking of Wind Turbine Sound by Ambient Noise

Karl Bolin

Stockholm 2006
Kungliga Tekniska Högskolan
School of Engineering Sciences
Department of Aeronautical and Vehicle Engineering
The Marcus Wallenberg Laboratory for Sound and Vibration Research

Postal address	**Visiting address**	**Contact**
Royal Institute of Technology	Teknikringen 8	Tel: +46 8 790 92 02
MWL / AVE	Stockholm	Fax: +46 8 790 61 22
SE-100 44 Stockholm		Email: kbolin@kth.se
Sweden		

Akademisk avhandling som med tillstånd av Kungliga Tekniska Högskolan i Stockholm framläggs till offentlig granskning för avläggande av teknologie licentiatexamen torsdagen den 14:e december 2006, kl 13.00 i sal MWL 74, Teknikringen 8, KTH, Stockholm.
TRITA-AVE -2006:86
ISSN -1651-7660

Abstract

Two aspects of ambient noise masking of sound from wind turbines are highlighted: the development of a prediction model for vegetation noise and the relative levels of ambient noise needed to mask wind turbine sound. The prediction model for vegetation noise has been compared with an earlier method with notable improvement, turbulent wind speeds are combined with the prediction model and a new model describing noise from deleafed trees are presented. A loudness test suggests that annoyance will occur at levels where the wind turbine noise exceed natural ambient noise by 3 dBA or more.

Licentiate thesis

This licentiate thesis consists of a summary and the appended papers listed below referred to as Paper A, Paper B and Paper C

Paper A K. Bolin 2006: "'Prediction method for vegetation noise"'

Paper B K. Bolin 2006: "'Influence of turbulence and wind speed profiles on vegetation noise"'

Paper C K. Bolin, S. Khan 2006: "'Determining the potentiality of masking wind turbine noise using natural ambient noise"', Submitted to *Acta Acustica*

Material from paper A and paper B have been presented at the conference Wind Turbine Noise 2005 in Berlin, Germany.

Division of work between the authors:
In paper C the theoretical and experimental work presented in the article, except for the analysis of variance, was performed by Karl Bolin under the supervision of Shafiquzzaman Khan. Both authors contributed to the writing of the article.

Contents

1 Introduction

Natural sounds have, since the beginning of our time, been a part of the environmental noise surrounding us humans. In rural areas the sound from wind flowing through vegetation would have been the dominating sound source, sometimes interrupted by human noise from craftsmen, a barking dog or bellowing cows. In coastal regions these sounds were accompanied by the sounds from waves breaking at the shorelines. This benign soundscape, constant for thousands of years, with the highest loudness produced by thunder or other rare natural phenomenas have since the beginning of the industrial revolution gradually become polluted by new artificial sound sources. The largest upheaval from the old rural soundscape came with the automobile, today a main noise polluter in Sweden [1] and in large parts of the developed world. This source has seriously altered the environment in many rural areas and further deterioration is indeed undesired. Today another emerging man made noise source are the wind turbine plants, these will grow in an increasing pace in the forthcoming years as signing states of the Kyoto protocol needs to fulfill their promises to decrease green house gases. This expansion will be particularly rapid in the offshore niche as large wind-farms are planned in several countries. This could lead to noise pollution along coasts and inside recreation areas, regions invaluable for recreational purposes for large populations.

The earliest major commercial wind turbine development was sited in California following the Oil Crisis in the mid 1970s. In the subsequent decade the first articles regarding noise annoyance from large wind turbines were published by Manning [2] and Hubbard et al. [3]. Much research has been conducted since these papers to arrive at the present knowledge level about wind turbine annoyance. In the early stages mechanical noise sources dominated. But improved sound isolation, e.g., rubber coated teeth in gearboxes and sound isolation of the nacelle have resulted in that present noise is mainly caused by broad band aerodynamic noise from the blades close to a turbine. This produce a distinct "swooshing" a sound similar to distant aircraft noise.

Different noise emission regulations exist in Europe, three basic strategies are the German, Dutch and British, respectively, which are described below. The German noise standard [4] allows for a noise imission of 45 dBA. This simple procedure will almost certainly result in suboptimal power output especially at higher wind speeds, because the ambient noise level usually increase faster than the turbine noise, thereby increasing the masking probability [5]. The Dutch noise regulation [6] adjust the allowed turbine limits depending on the wind speed, thereby it implicitly accounts for the masking by background sound. This result in a simple but coarse procedure as these standardized ambient noise levels should be set low to avoid annoyance. The assumption that ambient noise levels

are approximately the same in different locations could be valid in a homogenous landscape like the Dutch farmland but many other countries have larger deviations in the rural landscape resulting in large variations in noise levels at different locations. This would result in very tight noise emission limits and non-optimal output from wind turbines, thereby increasing the number of wind turbines to produce the same amount of electricity. The British assessment method [7] allows for 5 dB higher turbine sound level than the measured background noise levels at different wind speeds. This procedure will hopefully result in optimized power output without causing large disturbances at nearby dwellings. However, extensive measurements for all seasons have to be performed at every wind turbine project and hence this method can prove both time-consuming and expensive. These three different approaches have their advantages and disadvantages respectively, either suboptimal power output or time consuming and expensive.

Although daily perceived by a large part of the population a surprisingly small amount of research has been conducted in the field of sound generated from vegetation. Although measurements of ambient noise levels are performed on a routine basis only a small amount of these have explicitly investigated noise generation from trees rather than determining the sound level at particular locations. The report by Sneddon et al [8] examines the noise generation from mixed coniferous forests in California and all year measurements of vegetation noise were performed by Jakobsen and Pedersen in [5]. However, Fégeant proposed the first semi-empirical prediction model of vegetation noise in [9] and [10] valid for different tree species and vegetation geometries. This analysis was validated for cases of non-turbulent flow. Further work by Fégeant [11] stressed the importance of wind turbulence causing variations in the level of vegetation noise. However, measurements have only been performed at wind speeds of 7 m/s and below [10], confirmation of the theory above these conditions is considered necessary in order to predict the noise at higher wind speeds. Furthermore the analytical expressions in [9] are not suited to estimate noise fluctuations and complicated vegetation geometries. Therefore the semi discrete model presented in paper A in this thesis is superior, at least in these aspects. This model is coupled to a method producing time series of turbulent winds in paper B which satisfactory estimate the time fluctuations of vegetation noise. The question of when vegetation noise mask wind turbine sound were estimated by Fégeant [12] by calculating the detectivity index. However the obvious similarities between the broadband noise of vegetation and wind turbine sound, makes it interesting to apply modern psycho-acoustic models [13] [14]. Therefore a laboratory study has been performed in paper C to investigate the masking threshold and partial loudness of mixed ambient noise and wind turbine sound. Apart from the vegetation noise the masking potential of sea wave noise has also been studied, this is considered important due to the large wind farms planned in offshore locations all over Europe and since sea noise commonly dominate the coastal soundscape.

2 Summary of papers

Paper A- Prediction method for vegetation noise

A model describing the noise generation from vegetation is presented. The research by Fégeant [9] and [10] is refined to better agree with measurements. A semi discrete model is proposed, this approach is better suited to process time fluctuating wind, turbulence, compared to the analytical model presented by Fégeant. Furthermore complex vegetation sources can easily be modeled. Sound generation from trees without foliage ("'deleafed"') are added and an all year spectra for sound from deciduous trees is proposed. The non-leafed sound spectrum is characterized by flow acoustic dipole sources when wind flows through the canopy as can be seen in Figure 1.

A term is added to the coniferous sound model by Fégeant to account for the aero-acoustic dipole sources when the wind flow around the branches and also to account for structural vibrations in moving canopy elements. These adjustments improves the spectral resemblance between predictions and measurements and also allows for estimation of all year deciduous sound level predictions. When compared to the Fégeant model the new model shows higher accuracy to estimate measured results at three locations, especially in the low frequency region see Figure 2. This is an important property because the masking potential of low frequency sound could be estimated with higher accuracy. Validations of the new model have also been performed at five locations including two without foliage. Measurements at wind speeds up to 12 m/s are also reported and compared to predictions with satisfying results this can be seen in Figure 3.

Paper B- Influence of turbulence and wind speed profiles on vegetation noise

The vertical wind velocity profile is modeled according to [15] and the implications of a changing velocity profile is evaluated. Wind turbulence also depend on atmospheric conditions, the variance of turbulence intensity are four times higher at unstable than in stable conditions [16], the implication of this on vegetation noise is severe because the emitted sound pressure are scaled with $p_{eff} \propto u^{\chi}$, where χ is a wind speed coefficient varying between 1.5 and 2.7 for different tree species [9]. The turbulence characteristic is combined with a simulation method that produce space- and time- correlated wind velocity time series. These data are inserted into a semi-discrete vegetation noise model to produce vegetation noise predictions capable to account for turbulence and changing vertical velocity profile.

Vegetation noise measurements from three locations are compared with simulations. One- and three-dimensional turbulence models have been used for the simulations. The observed similarity between one dimension and three dimension turbulence models indicate that the turbulence perpendicular to the mean wind direction can be neglected when estimating fluctuations in vegetation noise. Satisfactory agreement between time variations in the measurements and simulations are shown, see table 1, this despite the relatively short measurement periods of 20 minutes. An estimation method of vegetation noise fluctuations proposed in [11] estimate the standard deviation of A-weighed sound pressure level by 6.2 dBA compared to performed measurements with standard deviations of 3.0 dBA and are therefore considered not accurate enough.

The papers conclusion is that atmospheric conditions and turbulence have large effect on vegetation noise. Modeling this sound source without accounting for these factors could result in serious misjudgment in the masking potential of vegetation sounds on disturbing noise sources. It is therefore suggested that accurate wind models, including turbulence, should be used when estimating vegetation noise according to the semi discrete model in paper A.

Paper C- Determining the potentiality of masking wind turbine noise using natural ambient noise

This article examines the masking potentiality of wind turbine noise in the presence of three natural ambient noises, namely vegetations (coniferous and deciduous) and sea wave noises. Four different listening tests were performed by 36 subjects. The first two tests determine the threshold of wind turbine noise in the presence of the natural ambient noise. The third test examine the perceived proportion of wind turbine and natural ambient noise at various S/N ratios (S is wind turbine noise and N is natural ambient noise). The last test investigate the partial loudness of wind turbine noise in the presence of natural ambient noise. Results of the threshold test showed that the average masking threshold varied from S/N-ratios of -5.3 dBA to -2.6 dBA, where coniferous noise revealed better masking potentiality than the other natural ambient noises (deciduous and sea wave). The third test showed that the proportion of wind turbine noise is perceived as less than 50% of the total noise at S/N ratios of 3 dBA and below. The partial loudness test indicated that the observed partial loudness was higher in all S/N ratios compared to the existing partial loudness model [13] [14].

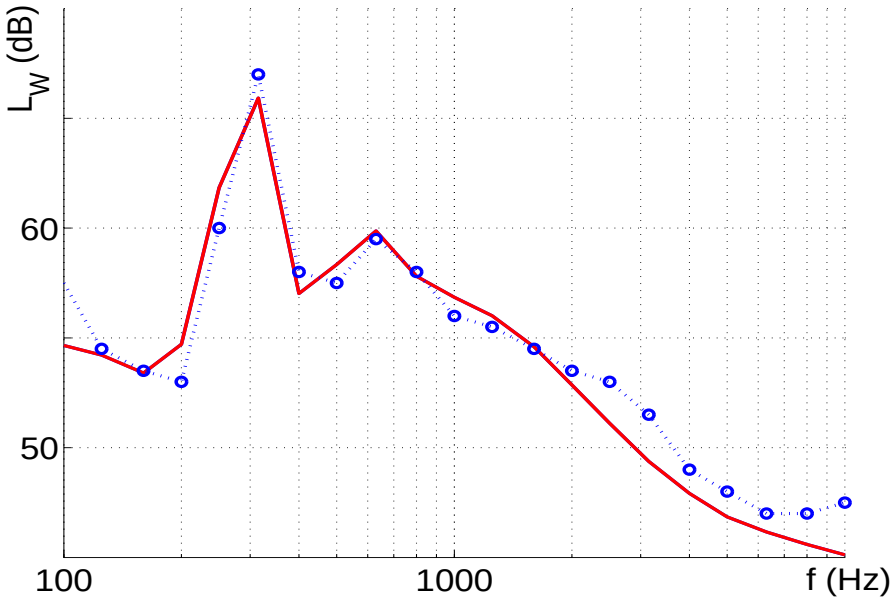

Figure 1: Third octave band noise spectra (sound power) in dB. Measurements (o) and prediction (—) for deleafed birch at a wind speed of 11.5 m/s. Note the peak corresponding to Strouhal-separation around the branches.

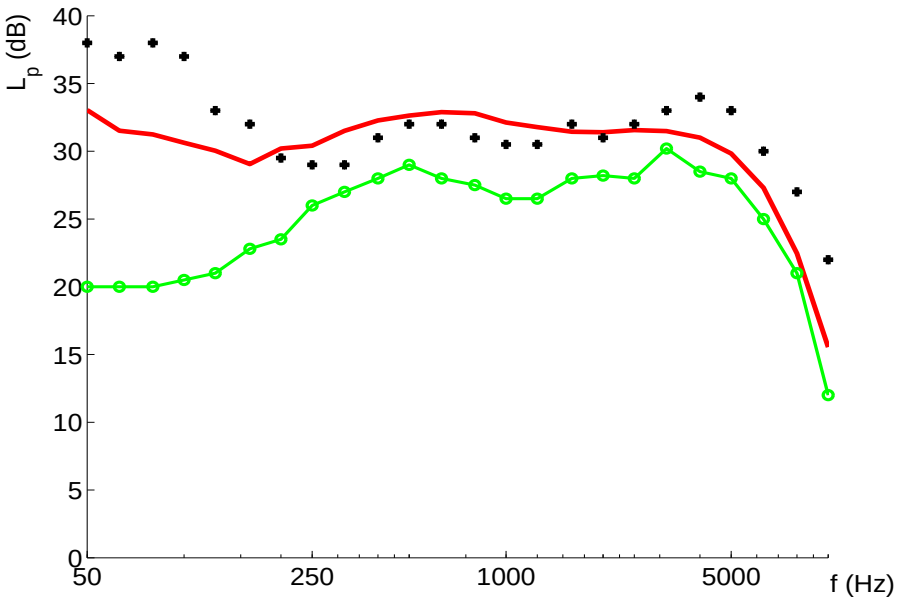

Figure 2: Sound pressure level in third octave bands at u =4.4 m/s. (•) Measurement, (—) Prediction by Bolin, (-•-) Prediction by Fégeant. Overview and third octave band sound pressure levels from the edge of aspens, site 5 in [17].

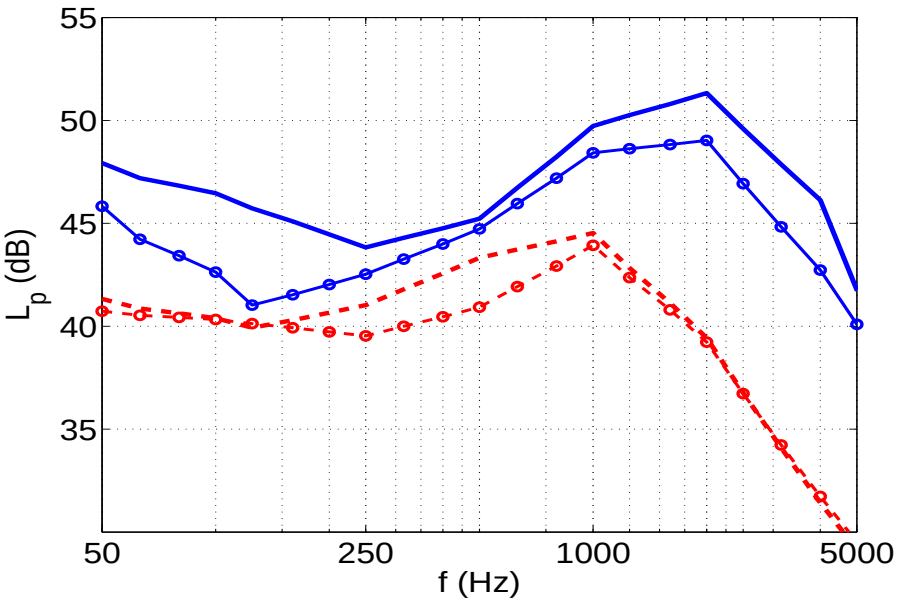

Figure 3: Third octave band spectrum of sound pressure levels. (-o-) measurements and (—) predictions respectively at u=8.3 m/s (—) and at u=4.6 m/s (- - -).

		Measurement		**3D Simulation**		**1D Simulation**	
		U (m/s)	L_A (dBA)	U (m/s)	L_A (dBA)	U (m/s)	L_A (dBA)
Site 1	$\bar{x}$	5.1	55.2	5.2	54.1	5.1	51.8
	σ_x	1.7	4.0	1.8	2.8	2.0	2.9
Site 2	$\bar{x}$	6.3	47.2	6.3	50.9	6.3	48.0
	σ_x	1.5	3.0	1.6	3.4	1.1	3.1
Site 3 Mic 1	$\bar{x}$	5.2	56.8	5.2	56.2	5.1	56.0
	σ_x	1.7	2.6	1.5	2.6	1.5	2.7
Site 3 Mic 2	$\bar{x}$	5.2	59.5	5.2	56.9	5.1	56.7
	σ_x	1.7	5.2	1.8	2.8	1.8	2.8

Table 1: Measured wind speed and sound levels, $\bar{x}$ denote average values and σ_x standard deviation.

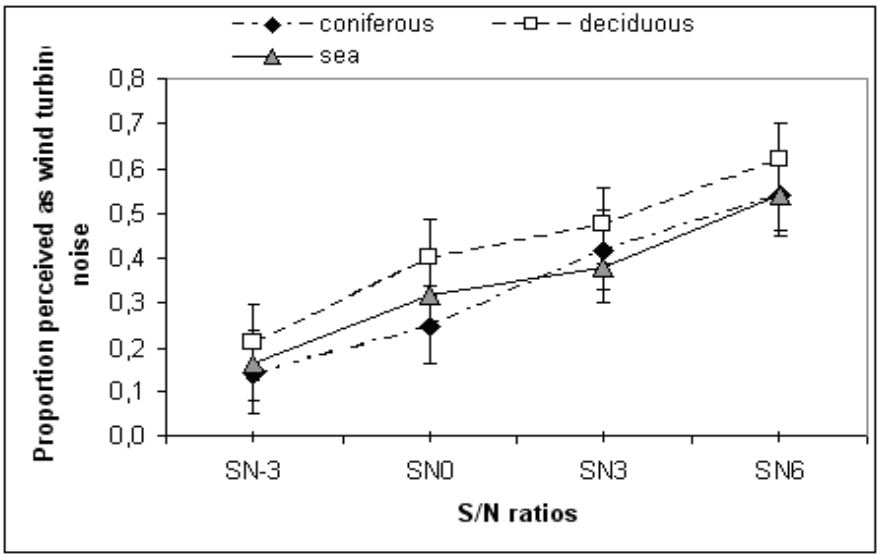

Figure 4: Proportion of sound perceived as wind turbine noise for different S/N-ratios, average values and confidence intervals of 95% are shown.

3 Future work

Future work consists in creating a semi-empirical model for predicting sea wave noise. This is considered important as offshore wind turbine farms are planned or already under construction in many parts of Europe. In the psycho-acoustic field tests to explicitly evaluate the annoyance should be performed and also a larger number of subjects should participate. In addition a new partial loudness model for wind turbine noise should be developed.

4 Acknowledgments

The financial support from the Swedish wind energy foundation (VINDFORSK) contract number 20134-2 is gratefully acknowledged. I would like to express my thanks to my supervisors professor Mats Åbom and associate professor Shafiquzzaman Khan for their guidance through the course of this project. My thanks also remain to my colleagues at the Marcus Wallenberg Laboratory. I am also grateful to my family and friends for their cordial support. Finally, I would like to thank Karin for making rainy days wonderful and sunny days even better.

References

[1] B Berglund and M E Nilsson. Total and source-specific loudness of singular and combined traffic sounds. Archives of the center for sensory research, 6(3) 2001.

[2] Manning P T. The environmental impact of the use of large wind turbines. *Wind Engineering*, 7(1), 1983.

[3] F W Grosveld H H Hubbard and K P Shepherd. Noise characteristics of large wind turbine generators. *Noise Control Engineering*, 21:21–29, 1983.

[4] TA-Lärm:. Technische anleitung zum schutz gegen lärm (technical guideline for noise protection). Technical Report Stand. GMBI. S. 503, Germany, 1998. (in German).

[5] J Jakobsen and T H Pedersen. Stoj fra vindmoller og vindstojens maskerende virkning. Technical Report 141, Lydtekniskt institut, Lyngby, 1989. (in Danish).

[6] A W Bezemer et al. Handleiding meten en rekenen industrielawaai (manual for measuring and calculating industrial noise). Technical Report 53-86, Den Haag, 1999. (in Dutch).

[7] R Meir et al. The assessment and rating of noise from wind farms. Technical Report ETSU-R-97, ETSU, Department of Trade and Industry, 1996.

[8] M Sneddon et al. Measurements and analysis of the indigenous sound environment of coniferous forests. Technical report, BBN System and Technologies, 1994. NPOA Report No. 91-1, BBN Report No.7210.

[9] O Fégeant. Wind-induced vegetation noise. part 1: A prediction model. *Acta Acustica*, 85:228–240, 1999.

[10] O Fégeant. Wind-induced vegetation noise. part 2: Field measurements. *Acta Acustica*, 85:241–249, 1999.

[11] O Fégeant. Masking of wind turbine noise: Influence of wind turbulence on ambient noise fluctuations. Technical Report 2002:12, Department of Civil and Architectural Engineering, Royal Institute of Technology, Sweden, 2002.

[12] O Fégeant. On the masking of wind turbine noise by ambient noise. In *European Wind Energy Conference, EWEC´99*, pages 184–188, 1999. Nice, France.

[13] B R Glasberg B C J Moore and T Baer. A model for the prediction of thresholds, loudness and partial loudness. *Journal of Audio Eng. Soc.*, 45:224–240, 1997.

[14] B C J Moore and B R Glasberg. A revision of zwickers loudness model. *Acta Acustica*, 82:335–345, 1996.

[15] Federal Ministry for Environment, Nature Conservation and Nuclear Safety, Bundesministerium für Umwelt, Naturschutz und Reaktorsicherheit. *TA-Luft, Erste Allgemeine Verwaltungsvorschrift zum Bundes-Immissionsschutzgesetzt- Techniche Anleitung zur Reinhaltung der Luft (First general directive to the federal immission protection act- Technical guideline for clean air)*, 2002. (inGerman).

[16] A Andrén. Evaluation of a turbulence closure scheme suitable for air pollution applications. *Journal of Applied Meteorology*, 29:224–239, 1990.

[17] O Fégeant. Wind turbine noise assessment. Technical report, Building Acoustics, KTH, Stockholm, 1997. TRITA-BYT 97/175.

Prediction method for vegetation noise

Karl Bolin
Royal Institute of Technology / Marcus Wallenberg Laboratory
Teknikringen 8
SE-100 44 Stockholm
Sweden
+46-(0)8 790 92 02
kbolin@kth.se

Abstract

This article examines the sound from vegetation generated by the wind. A new method for predicting sound from deleafed trees has been combined with improvements of an earlier model enabling the possibility to predict vegetation noise at all leaf densities. The proposed prediction method and an earlier model have been compared with measurements which show improved agreement, in particular in the region below 1 kHz at three locations. Comparisons between 5 new measurement sites and predictions show satisfying agreement. The model is verified for wind speeds of 12 m/s.

1 Introduction

As noise disturbance is becoming an accentuated problem in many rural regions the need for correct estimations of the perceived annoyance are increasing. In many areas the ambient noise level is considered to consist mainly of sound from natural sources which are perceived as less disturbing than artificial noise. Hence this article aim at presenting a prediction model of one of the most common natural sounds, that from vegetation. This could be used to estimate the masking potential of vegetation noise on different man made noise sources.

Although daily perceived by a large part of the population a surprisingly small amount of research has been conducted in the field of sound generated by vegetation. Fégeant proposed a semi-empirical analytical prediction model of vegetation noise in [1] and [2] for different tree species and vegetation geometries. This analysis was validated for cases of non-turbulent flow. Further work by Fégeant [3] stressed the importance of wind turbulence causing variations in the level of vegetation noise. However, the number of measurement sites were limited and measurements have only been performed at wind speeds of 7 m/s and below. Confirmation of the theory above these conditions is considered necessary in order to be able to model the noise at higher wind speeds.

The objectives of this article are to improve the Fégeant model, to predict the emitted sound with higher accuracy and discuss the acoustical phenomenas that might explain the shortcomings of the earlier model. A new model is suggested to estimate sound from deleafed trees and intermediate states between trees with or without foliage. The analytical expressions from [2] have been replaced by discrete equivalents, better suited to deal with increased complexity of the terrain. Comparisons between the two models and new measurements are also presented. Also measurements of vegetation noise have been performed at five locations at high wind speeds not previously reported in the literature. Comparison between predictions and measured results shows good possibilities to estimate noise from vegetation.

2 Vegetation noise

2.1 Fégeants model

The semi-empirical analytical model developed by Fégeant [1] and [2] is to the authors knowledge the most complete prediction method of vegetation noise published. The effective acoustic pressure fluctuations were calculated by

$$p_{eff}^2(f) = \frac{\rho c}{4\pi} \iiint_V dW(f, \mathbf{r}) J(f, \mathbf{r})\, dV \tag{1}$$

where f [Hz] is the sound frequency, $\mathbf{r}$ [m] is the vector from the source to the receiver, ρ [kgm^{-3}] is the air density, c [ms^{-1}] the sound speed, dW [Wm^{-3}]the sound power emitted by volume element dV [m^3] and $J(f, \mathbf{r})$ [m^{-1}] the propagation factor from a spherical sound source.

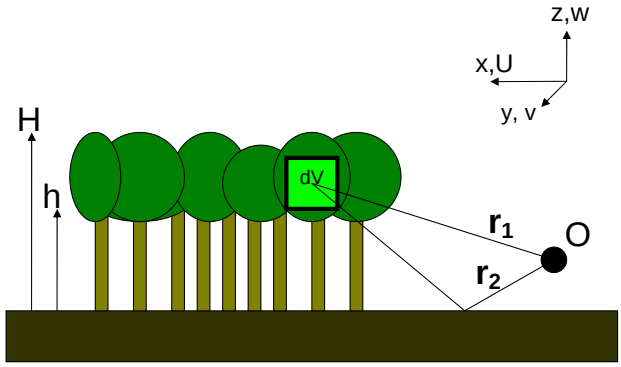

Figure 1: Geometry of vegetation with tree height H, trunk free height h, volume element dV, propagation paths $\mathbf{r_1}$ and $\mathbf{r_2}$ to observer position $\mathbf{O}$. In the upper right corner the Cartesian coordinates (x, y, z) where x correspond to the mean wind direction with wind speed $\mathbf{U}$, y is the horizontal direction orthogonal to x and z is the vertical direction with their respective wind components v and w.

The function $J(f, \mathbf{r})$ shown in equation (2) represents the propagation of a spherical sound source along the rays $\mathbf{r}_1$ and $\mathbf{r}_2$ shown in Figure 1. It can be written as

$$J(f, \mathbf{r}) = \left| \frac{e^{-\alpha r_1}}{r_1} + R \frac{e^{-\alpha r_2}}{r_2} \right|^2 \tag{2}$$

where the α is the attenuation coefficient calculated according to ISO 9613 [4] and the phase could be disregarded as explained by Fégeant in [1]. R is the ground reflection coefficient calculated as described by Delany and Bazeley in [5] with ground impedance values from Nord 2000 [6].

In equation (1) the acoustic power from volume element dV is calculated by

$$dW(f, \mathbf{r}) = A \cdot S(\mathbf{r}) \Gamma(f) U^{2\chi} \tag{3}$$

where A is a radiation constant with changing dimension, $S(\mathbf{r})$ [m^2/m^3] is the leaf area density defined as "the total one sided leaf area per unit of ground surface and unit of height [m^2/m^3] this parameter varies for different tree species [7] [8] [9], U is the wind speed and χ is the wind speed coefficient. These parameters are described in detail in [1]. The unit of the radiation constant A could be made constant by replacing U with the Mach number $M = U/c$. The dimensionless frequency spectra $\Gamma(f)$ are separated into coniferous and deciduous species. In the coniferous case it is described by

$$\Gamma_c(f) = e^{-\lambda log^2(\frac{f}{f_c})} \tag{4}$$

where λ determine the width of the spectrum, f_c [Hz] is the Strouhal frequency, expressed as

$$f_c = St\frac{U}{d_n} \tag{5}$$

with the Strouhal number $St = 0.2$, U (m/s) is the wind velocity and d_n (m) is the needle diameter shown in table 1.

Species	$A \times 10^{-13}$	χ	$d_n \times 10^{-3}$[m]	λ
Pine	6	1.8	1.3	10
Spruce	3.5	1.5	1.0	15

Table 1: Parameters for coniferous species.

For the deciduous species the spectrum is given by equation (6)

$$\Gamma_d(f) = C_1 f^{-1} + C_2 e^{-C_3\frac{(f-f_d)^2}{f_d^2}} \tag{6}$$

The coefficients C_n and f_d (Hz) are described in [2] and are shown in table 2. The first term in this equation represent a pink noise term which describe the low frequency sound emission from deciduous trees and the second part describe the noise originating from colliding leaves.

Species	$A \times 10^{-13}$	χ	C_1	C_2	C_3	f_d (Hz)
Birch	1.6	1.8	932	0.8	2	4500
Aspen	10	2.7	120	1.0	1	3200
Oak	0.44	1.8	1580	0.5	1	3000

Table 2: Parameters for deciduous species.

2.2 Proposed model

Although innovative, the work of Fégeant [1] and [2] shows some limitations, the following improvements are obtained using data reported in [1], [2] and [10]. The most obvious inadequacy can be observed in the deciduous trees at deleafed conditions, that is when

$$\lim_{S \to 0} dW = 0 \tag{7}$$

consequently vegetation without leafs or needles does not generate sound in this model. This omits the sound generated by the stem, branches and twigs. It is therefore suggested that the spectrum in formula (3) are separated to a term describing the sound from leafs and another accounting for the sound from branches etc.

$$\Gamma(f, S) = \frac{S}{S_{max}} \Gamma_d(f) + \frac{S_{max} - S}{S_{max}} \Gamma_{dl}(f) \tag{8}$$

where S_{max} is the fully leafed leaf area density from [7] [8] [9]. The frequency spectrum $\Gamma_d(f)$ is acquired from equation (6). However, the contribution of $\Gamma_d(f)$ is linearly depending on the leaf area density S to enable $\Gamma(f, S)$ to transform into the deleafed model $\Gamma_{dl}(f)$ presented later in this article.

2.2.1 All year deciduous spectrum

Fégeant measured the sound power from a deleafed birch in [10] but no model of the sound generation in this state was presented. However, as this will be the condition for large parts of the year it is considered important that a prediction method of deleafed deciduous trees exist if all year predictions of vegetation noise are to be performed.

The main sound sources from a deleafed tree is assumed to be an aero-acoustic dipole source when wind is flowing round the branches and twigs and mechanical induced vibrations when collisions between canopy elements occur. In this article the sound generation from mechanical vibrations is modeled as a pink noise term depending on the leaf area density. At deleafed conditions the increased porosity in the canopies should cause smaller motions in the foliage, thereby decreasing the number of collisions and consequently changing the sound spectrum. In this state the aero-acoustic dipole sources should be increasing in intensity, as they are depending on the wind speed and diameters of the branches and twigs. The diameter distributions are here assumed constant for all tree species, therefore

only one model is needed for all deleafed trees. The peaks in the Figure 2 are modeled by three dipole components as shown in equation (9)

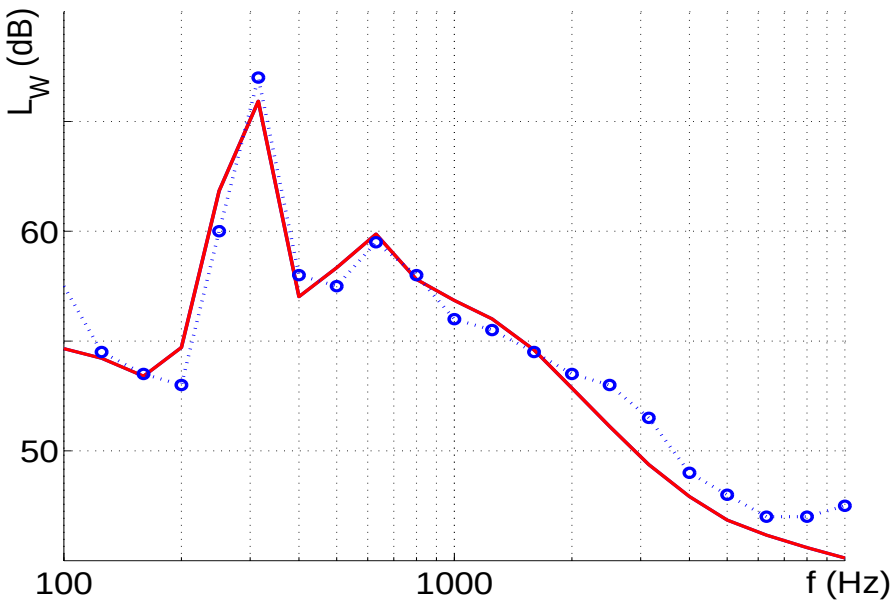

Figure 2: Third octave band noise spectra in dB of measurements (-o-) from [1] and prediction (—) for deleafed birch at a wind speed of 11.5 m/s.

$$\Gamma_{dl}(f) = C_4 f^{-3} + \sum_{i=1}^{3} C_{5i} e^{-\lambda_i log^2\left[\frac{f}{f_i}\right]} \qquad (9)$$

$$f_i = St\frac{U}{d_{bt\,i}}$$

where $C_4 = 10$ and C_{5i} are constants, λ_i are parameters describing the width of the spectrum and $d_{bt\,i}$ are the diameters of the branches and twigs. The values of these coefficients are presented in table 3, these are acquired from a least squares approximation of the third octave band measurements shown in Figure 2.

i	C_{5i}	λ_i	$d_{bt\,i}\ \times 10^{-3}$(m)
1	25	700	7.5
2	1	300	3.7
3	1	6	5

Table 3: Parameters of equation (9)

From Figure 2 it can be observed that there are two peaks, at 300 Hz and 600 Hz, these are probably related to the branches diameter distribution having peaks at d_{bt} =7.5 mm and 3.7 mm, this distribution is unfortunately not described in known literature but from observations of deleafed birches the two peaks in diameter distribution described above seems reasonable. The remaining branches and twigs are estimated by the first term, $C_4 \cdot f^{-3}$ and the third dipole source that consequently has a much broader peak modeled by the parameter λ_3 in equation (9).

2.2.2 Coniferous spectrum

The coniferous spectrum derived by Fégeant in [1] have a single sound generating mechanism, the dipole source created when the air flows around the needles. As a consequence, the predictions seen in Figure 3 show very large estimation errors in the low frequency domain. It is believed that these low frequency sound levels could be explained partly by structural vibrations caused when the canopy elements collide and by dipole sources from branches and twigs. Therefore a term is added to equation (8) as shown in equation (10).

$$\Gamma_c(f) = e^{-\lambda\, log^2(\frac{f}{f_c})} + C_c e^{-\lambda_2 log^2(\frac{f}{f_2})}$$
$$f_2 = St\frac{U}{d_{bt}} \tag{10}$$

where the coefficients λ and f_c are acquired from equation (4), C_c, λ_2 and d_{bt} are estimated by least squares approximation of the measurements shown in Figure 3 and are shown in table 4. The evergreen coniferous trees will show smaller seasonal variations in the sound spectrum and are therefore assumed independent of the needle area density S which is approximately constant over different seasons.

Species	C_c	λ_2	$d_{bt}\,(m)$
Pine	100	0.50	0.03
Spruce	100	0.16	0.20

Table 4: Table of parameters of equation 10

The λ values in the coniferous spectrum Γ_c in equation (4) are depending on wind speed, as observed in [10], however these factors were assumed constant in order to simplify the analytical calculations. In this paper the parameters are linearized with respect to wind speed according to

$$\lambda_{pine} = -0.58U + 13.6$$
$$\lambda_{spruce} = -1.15U + 23.3 \tag{11}$$

This results in wider spectral peaks increasing with wind speed as can be seen in Figure 3 where the spectrum of the proposed model and the Fégeant spectrum are compared to measurements. These diagrams shows better resemblance between the measurements and the new model compared to the old, in particular in the frequencies below 400 Hz for the low wind speed case and below 1 kHz at the higher speed.

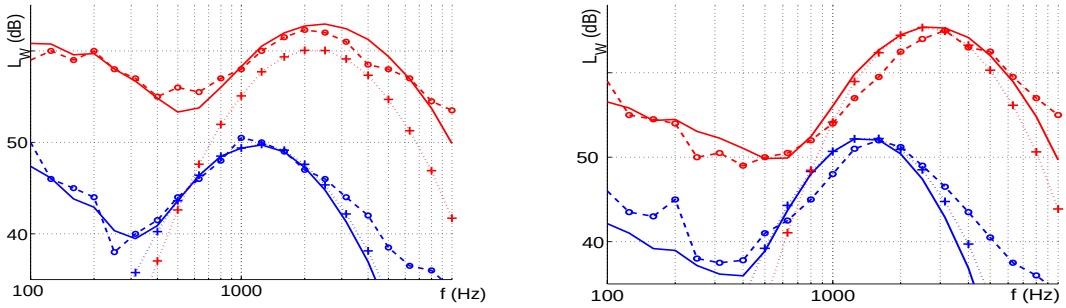

(a) Pine (b) Spruce

Figure 3: Acoustic power in third octave band noise spectra (dB) from coniferous species, wind speed 6.3 m/s , lower curves, and 11.5 m/s, upper curves. (**- o -**) Measurements, (—) predictions by new model and (- + -) predictions by Fégeant model.

2.2.3 The semi discrete model

The Fégeant model is analytical, thereby not optimally suited to combine with the indeterministic nature of wind turbulence which is preferably modeled by a random process. To circumvent this predicament a discrete vegetation noise model is advantageous as it could be combined with a stochastic turbulence model in order to evaluate the fluctuations of vegetation sound caused by variations of wind speed. The emitted power ΔW_{mn} from the surface element ΔS_{mn}, where (m, n) represent the discrete indices in the (x, y) horizontal directions, can be written as

$$\Delta W_{mn} = C_R \, M^{2\chi} \cdot \Gamma(f, S) \tag{12}$$

where C_R with the unit $(\mathrm{W/m^3})$ is the species dependent radiation constant shown in table 5 and χ the wind speed coefficient from [1].

	Birch	Aspen	Oak	Pine	Spruce	Deleafed
$C_R \cdot 10^{-13}$	3.2	10	0.88	3.4	2	3.3

Table 5: Table of radiation constant $C_R(W/m^3)$

The pressure fluctuations can now be calculated by

$$p_{eff}^2(f) = \frac{\rho c}{4\pi} \sum_{m=1}^{M} \sum_{n=1}^{N} J_{mn}(f, \mathbf{r}) \int_{z=h}^{H} \Delta W_{mn} dz \, \Delta x \, \Delta y \tag{13}$$

Discretization step size in the (x, y)-plane are set to 2 m, at this size the predicted sound pressure level converge for both extended sources, e. g. forests and forest edges, and compact sources, e. g. single trees and shelterbelts. The analytical integration with respect to z are performed to decrease the needed number of calculations. To limit the number of calculations performed when extended sources are simulated vegetation further away than $10 \cdot H_{max}$ are disregarded where H_{max} is the highest vegetation in the simulation.

2.3 Comparison between the models

When comparing measurements and predictions by Fégeant to the suggested model some factors have mainly been considered. Firstly, Fégeant used some of his measurement sites for parameter calibration, these are disregarded as they might bias the comparison. Secondly different tree species and wind speeds should be evaluated to give results with general validity. Therefore, this section presents measurements and predictions reported in [10] which are compared to the proposed model. The ground configuration are assumed to be grass and the microphone is at 1.4 m above the ground in all measurements. The meteorological parameters are not mentioned in [10], hence a temperature of 20°C and a relative humidity H_R of 70% have been assumed in the simulations with the new model.

Edge of aspens: This forest edge consisted of aspens with the height of 17 m and the trunk free height of 8 m. The microphone was placed at 50 m distance from the edge as shown in Figure 4(a). This location is denoted site 4 in Fégeant [10].

In Figure 4(b) it is observed that the new model estimates the measurements with higher accuracy in the frequency bands f <100 Hz and 500 Hz< f <3000 Hz but fails to predict the decrease around 250 Hz, which might be explained by ground effects, however the new method improve the estimation at 15 of 24 third octave bands.

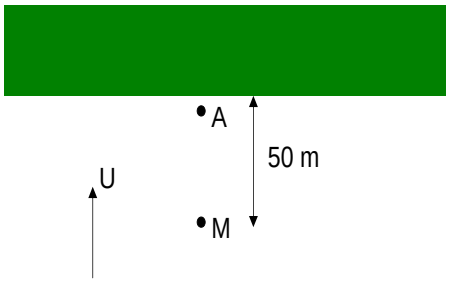

(a) Overview of anemometer (A), microphone (M) and the wind direction (U). The vegetation is denoted by the dark field.

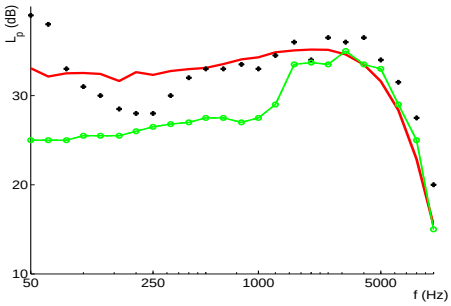

(b) Sound pressure level in third octave bands at $U = 3.3\,ms^{-1}$. (•) Measurement, (—) Prediction by Bolin, (-•-) Prediction by Fégeant.

Figure 4: Overview and third octave band sound pressure levels from the edge of aspens.

Edge of mixed species: This is, as the previous location, a forest edge shown in Figure 5(b). The vegetation consisted of spruce (1), pine (2) and aspen (3) with common height H=10 m, the three aspens were approximately 4 m in diameter. The microphone was placed 40 m from the edge. This location is enumerated site 5 in [10]. The geometry of the site is sketched in Figure 5(a).

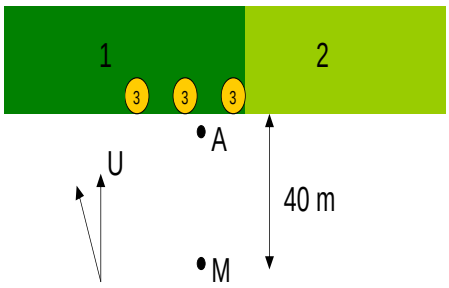

(a) Overview of anemometer (A), microphone (M), wind mean velocity (U) and vegetation position. Region 1 consist of spruce, the area denoted 2 consisted of pines and in the regions denoted 3 were aspens.

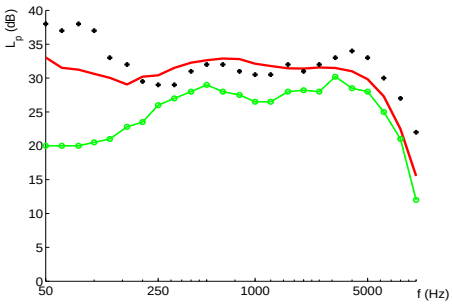

(b) Sound pressure level in third octave bands at $U = 4.4\,ms^{-1}$. (•) Measurement, (—) Prediction by Bolin, (-•-) Prediction by Fégeant.

Figure 5: Overview and third octave band sound pressure levels from the edge of aspens.

The sound levels at this site is also estimated with higher accuracy by the new model, as can be seen in Figure 5(b), especially in the low frequency region. The Fégeant model underestimate the sound level at 100 Hz by 18 dB compared to the new estimation where the error is 7 dB. The large misjudgment of low frequency noise could either be explained by vegetation

noise from sources at larger distances which is not modeled or by other background noise sources.

Edge of spruces: The location consisted of mainly spruces with two oak trees close to the microphone and is shown in Figure 6(a). The heights of the trees were approximately 15 m and the trunk free height were 0 m for the spruces and 2 m for the oaks, the oaks diameters were 4 m. The microphone was placed 27 m from the edge. The spectrum in Figure 6(b) shows a typical conifer vegetation source with a frequency top around 400 Hz. The new model shows higher accuracy compared to the Fégeant model, particularly in the low frequency region.

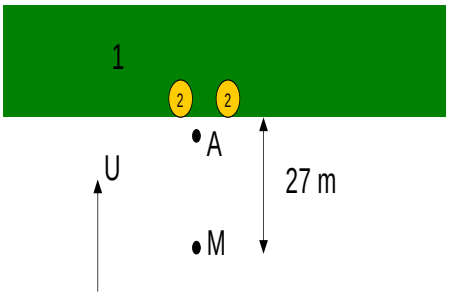

(a) Overview of anemometer (A), microphone (M), wind mean velocity (U) and vegetation position. The main region, 1, consisted of spruce and the two oak trees are denoted 2.

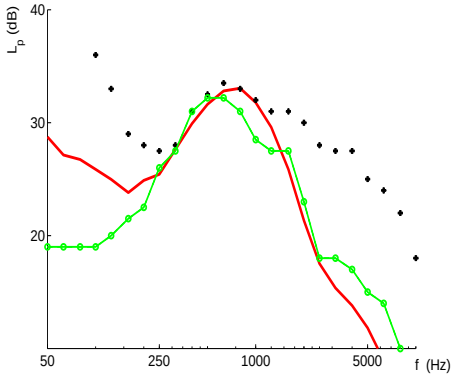

(b) Sound pressure level in third octave bands at $U = 2.5m/s$. (•) Measurement, (—) Prediction by Bolin, (-•-) Prediction by Fégeant.

Figure 6: Overview and third octave band sound pressure levels from the edge of aspens, site 7 in [10].

The conclusion from the comparisons shown above is that the new model predict the low frequency sound generation by vegetation better than the model suggested by Fégeant. The effect of this improvement could be considered minor when estimating the total sound pressure level, especially if this is A-weighed. However when masking potential by vegetation noise on low frequency noise are examined the consequence of this change could be large. The underestimations still existing in the new model could probably be explained by vegetation sources at greater distances or by other noise sources.

3 Measurements

To investigate the sound generated by vegetation at higher wind speeds and in the non-leafed conditions of deciduous trees new measurements were considered necessary. Measurements were conducted in agreement to the procedure described in ISO 1996 [11]. The measurement setup consisted of a cup anemometer mounted on a 10 m high pole, and a weather station registering humidity and temperature. The sound measurement equipment consisted of 1/2" microphones at 1.2 m height above ground connected to a digital analyzer SONY PC216Ax. In order to decrease the pseudo-noise generated by wind the microphones were protected by a foam windscreen 10 cm in diameter, the sound damping produced by the protection are corrected in the analysis of the measurements. Further precautions to reduce the pseudo-noise at the third measurement location where a high pass filter with a cutoff frequency of 20 Hz was used. At the last two sites a foam windscreen, with a height and width of 80 cm and depth of 11.5 cm was applied 0.5 m upwind from the microphone to reduce the pseudo-noise, the damping produced by this were not effecting the vegetation noise at neither site as the vegetation were downwind from the microphone at both locations. The distance between the microphone and windscreen is considered long enough to reduce possible reflections from the windscreen. In these two locations the anemometer was mounted in the tree canopies at 5 m and 4 m height and the wind speed extrapolated at 10 m height according to the German standard "'TA-luft"' [12]. The vertical velocity profile is unaltered at the vegetation edges as shown by Miller [13]. In the deleafed case trees have higher porosity than trees with foliage and therefore the conclusion by Miller should also be valid in the deleafed canopies. Recordings were performed in the frequency range from 43.2 Hz to 11.2 kHz with a sampling frequency of 48 kHz.

3.1 Description of sites

When choosing measurement locations some main aspects have been taken into consideration. The first and most important factor is the absence of other noise sources (primarily traffic- and aircraft noise). It is also favorable if sites have vegetation sources with similar tree species and tree height. One dominant sound source, for example a single large tree or a forest edge, is also considered positive. All measurement locations except site 3 fulfill the first condition. At that location a wind turbine Vestas 52 was situated a distance of 0.8 km downwind from the measurement location. The emphasis in these measurements have been to examine coniferous species as these species constitute 85% of the forests in Sweden. The last two sites are investigating how the deleafed model correspond to outdoor measurements. Measurements have also been performed at higher wind speeds

compared to earlier reported measurements, this was considered important in order to verify the model in these conditions.

3.1.1 Site 1

The measurement equipment were mounted close to a forest edge consisting of spruces of mixed height. The location geometry and a photograph are shown in Figure 7. The region denoted 1 was 120 m wide and 30 m deep and consisted of spruces with height H_1=12 m and a trunk free height h_1=1 m. Region 2 consisted mainly of spruces with a height H_2=5 m and a trunk free space h_2=0.5 m. The microphone (M) and anemometer (A) was positioned 29 m from the forest edge and the ground consisted of grass. Meteorological conditions were as follows: wind direction was perpendicular to the forest edge, temperature T=10°C, relative humidity H_R=82%, atmospheric pressure was not measured and is approximated to 1 atm.

(a) Vegetation geometry and equipment setup of site 1.

(b) Photography of site 1

Figure 7: Geometry and photography of forest edge of spruces, site 1.

3.1.2 Site 2

This location, see Figure 8, was dominated by a single spruce, denoted 1 in the figure with an estimated height of 18 m and a trunk space height of 2 m. Downwind of this tree a pine was standing with a height of 15 m and a trunk space of 8 m. This tree is denoted region 2 in Figure 8. Upwind of the spruce a shrubbery of junipers and spruces were growing, these are modeled as spruces in the simulations as the needle diameter should be similar. The anemometer (A) and the microphone (M) were placed at distances of 5 m and 3 m from the spruce. The ground was covered with grass. The temperature was 11°C and the relative humidity was measured to 100% caused by a dizzle.

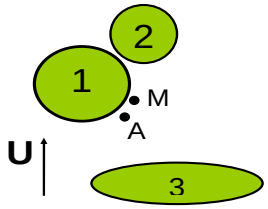

Figure 8: Geometry of the compact source, site 2. Unfortunately no photograph from this location is available.

3.1.3 Site 3

At this location a hedge of birches (1) with a depth of 5 m and a length of 45 m were located a distance of 100 m from the measurement equipment, see Figure 9. The height of the birches was estimated to H_1=20 m and the trunk free space to h_1=1 m. The site was dominated by an edge of mixed conifers region 2 consisting of both pines and spruces as can be seen in Figure 9(b) with tree height H_2=20 m but the trunk height differed $h_{2,p}$=7 m and $h_{2,s}$=2 m for pine and spruce respectively. The width of the forest was 155 m and the depth was several hundreds of meters thereby the approximation that only the region between the forest edge and $2H$ inward contribute to the noise generation [1] is valid. There were shrubberies of hazel below the trees; these are however not modeled in the simulations. By the side of the forest edge there was a L-shaped hedge, region 3, of birches at a distance of 40 m from the microphones. These trees were 20 m high and had a trunk height of 1 m. Both legs of the hedge were 30 m long and with a width of 3 m. The ground was covered with short grass. Two microphones were used, the first M_1, placed 10 m upwind of the forest edge and the second M_2 placed at the edge close to the anemometer A. The temperature was T=25°C and the relative humidity H_R=50%. A wind turbine type Vestas V52 was standing at a distance of 0.8 km from the site in the direction of hedge 1 which might contribute to the low frequencies in the measurements.

3.1.4 Site 4

The measurement location was close to a group of three deleafed birches, as seen in Figure 10. Around 50 m from the microphone, a forest of spruces was located, results from these measurement has therefore been chosen at gusts when the wind speed was high compared to the average wind speed. Unfortunately this procedure leads to short measurement periods but that the measured noise originate mainly from the deleafed vegetation is considered advantageous. The tree heights were 17 m, 12 m and 17 m respectively and the trunk free space were 3 m, 2 m and 2 m at tree 1, 2, and 3 in Figure 10(a). The temperature

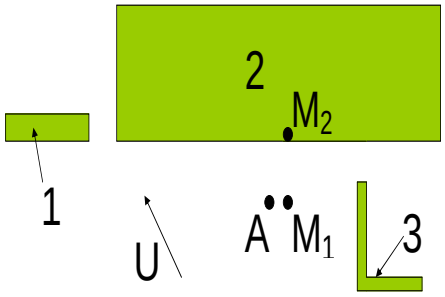

(a) Vegetation geometry and equipment setup of site 3.

(b) Photography of site 3

Figure 9: Geometry and photography site 3.

was 16°C and the humidity 24%. The ground configuration was long dried grass which caused high frequency noise.

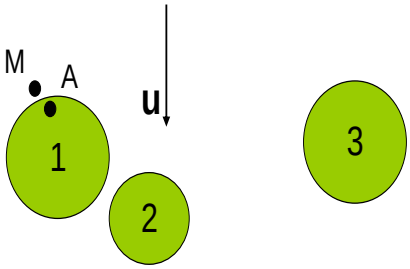

(a) Vegetation geometry and equipment setup of site 4.

(b) Photography of site 4.

Figure 10: Geometry and photography site 4.

3.1.5 Site 5

This site consisted of a group of deleafed alders in a region 40 m long and 15 m wide, as seen in Figure 11. The tree height were 18 m and the trunk free height 0 m. A brook was flowing through the vegetation at a distance of 6 m to the microphone. The flow in the brook was calm and steady therefore the noise from this source is assumed negligible. The temperature was 14 °C and the humidity was 24%. The microphone was placed 2 m upwind from the vegetation edge. Also at this location high dried grass caused high frequency noise.

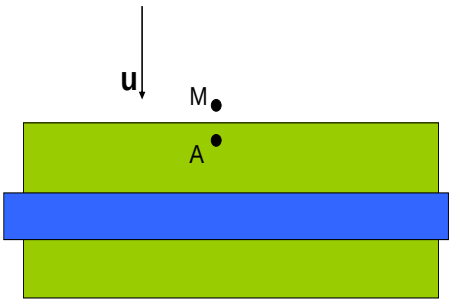

(a) Vegetation geometry and equipment setup of site 5. The creek is sketched by the rectangle in the central part.

(b) Photography of site 5

Figure 11: Geometry and photography site 5.

3.2 Model validation

This subsection present measurement results and model predictions from the locations described above in section 3.1. The section is separated into two parts, the first concerns the coniferous measurement locations and the second is about the sites with deleafed trees.

In order to examine the spectral accuracy of the coniferous prediction model third octave band sound pressure levels of measurements and predictions from site 1 and 2 are shown in Figure 12 and for site 3 in Figure 13. The tendency to underestimate the low frequency bands noted in section 2.3 remains and might be explained by the presence of noise from vegetation at longer distances or by pseudo-noise. The estimations are seen to be quite accurate, especially for site 1 and 3 but somewhat inaccurate in the compact source case, site 2. Possible explanations for the error at this site could be estimation errors in the simulations either by the height or by the horizontal extensions of the tree canopies. Another possible reason could be that the wind direction was rotating from the mean wind direction causing less sheltering of the pine behind the spruce which should increase the width of the sound level peaks as pine needles are thicker and hence the peak frequency lower compared to spruces. A combination of the causes mentioned above is naturally also possible.

The third octave band spectrum from site 4 and 5 are shown in Figure 14. It can be observed that the Strouhal frequencies of the branches and twigs are shown at site 4 as distinct peaks. The discrepancies of the low Strouhal frequency at site 5 might be explained by different diameters of the twigs at aldens compared to birches. The measured sound above 1 kHz should originate from the tall grass present near the microphones in both sites as this was noted to cause considerable high frequency noise during the measurement. The contribution by pseudo-noise seems to have decreased in these two spectra compared to the former sites. This

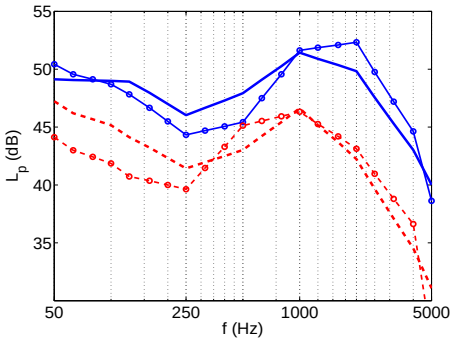

(a) Site 1 at U=8.5 m/s (—) and at U=6.1 m/s (- - -).

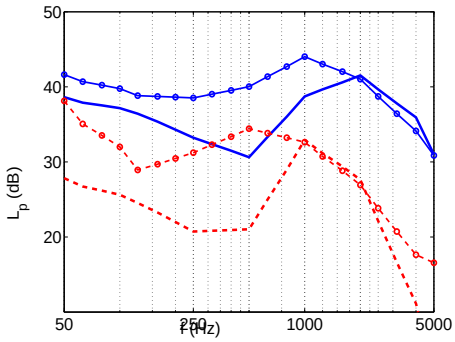

(b) Site 2 at U=8.5 m/s (—) and at U=4.8 m/s (- - -).

Figure 12: Third octave band spectrum of sound pressure levels. (-o-) measurements and (—) predictions respectively.

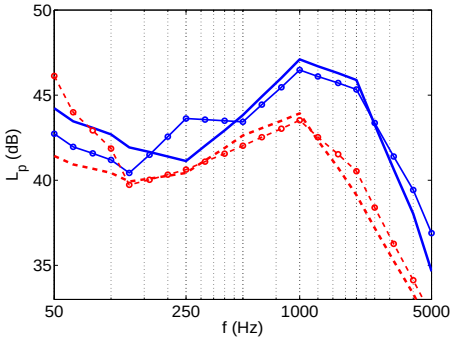

(a) Site 3 Microphone 1 at U=6.8 m/s (—) and at U=4.6 m/s (- - -).

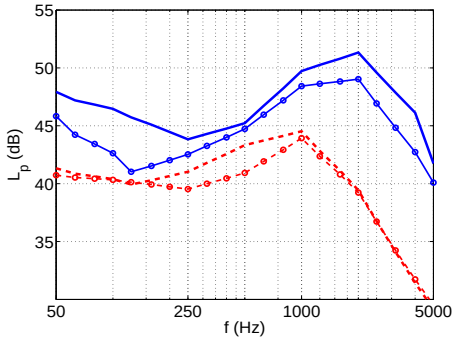

(b) Site 3 Microphone 2 at U=8.3 m/s (—) and at U=4.6 m/s (- - -).

Figure 13: Third octave band spectrum of sound pressure levels. (-o-) measurements and (—) predictions respectively.

could be explained by the lower flow behind the foam windscreen.

3.3 Wind speed dependence

Vegetation noise is obviously caused by the wind slowing through the canopies, however the relationship between wind speed and sound generation have been modeled differently in the Fégeant model [1], [2] and in a technical report by Sneddon et al. [14]. Thereby it is considered interesting to examine how the vegetation noise depend on the wind speed. In Sneddon et al. [14], a vast number of A-weighed sound pressure levels from measurements inside coniferous forest are correlated to their respective wind speeds. The sound level is estimated as a linear function of wind speed, $L_A = AU + B$. This hypothesis by Sneddon

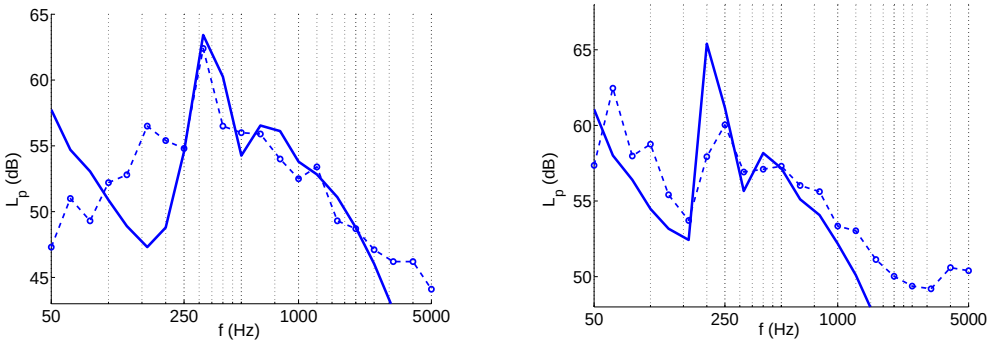

(a) Site 4 -o- and — measurements and predictions at U=8.0 m/s.

(b) Site 5 -o- and — measurements and predictions at U=12.0 m/s.

Figure 14: Third octave band spectrum of site 4 and site 5 respectively.

is here compared to the curve fitting by Fégeant [1] who proposed $p_{eff} \propto U^{\chi}$ dependence for the peak sound pressure. The Sneddon assumption obviously encounters problems when

$$\lim_{U \to 0} W \neq 0 \tag{14}$$

which contradict the natural boundary condition that without airflow no vegetation noise is generated. It is probable that the Fégeant dependence should yield better estimations of the wind speed dependence because these tests are performed in a wind tunnel with a controlled and coherent airflow. Also the signal to noise ratio is higher compared to the field measurements in the Sneddon report where the wind field is not completely known and background noise most probably exists. However, it should also be observed that all of Fégeant´s estimations underestimate the generated sound power at higher wind speeds see Figure 15, suggesting that this approach to the sound power level contra wind velocity may not be valid in this region.

When estimating the wind speed dependence both Sneddon and Fégeant used measured sound pressure levels as a function of wind speed in similar ways as shown in Figure 15 where A-weighed sound pressure levels are given for the three first measurement locations as a function of wind speed. From these figures the wind speed dependence can be calculated by least square fits as shown in the graphs. However, most measurement points are concentrated around the average wind speed and therefore curve fitting algorithms will bias the approximation in favor of this wind speed region and therefore extreme wind speeds will be judged less important. This algorithm allow large errors at wind speeds with few measurement points and is therefore considered inadequate.

To evaluate the wind speed dependence with higher accuracy 10% of the sound

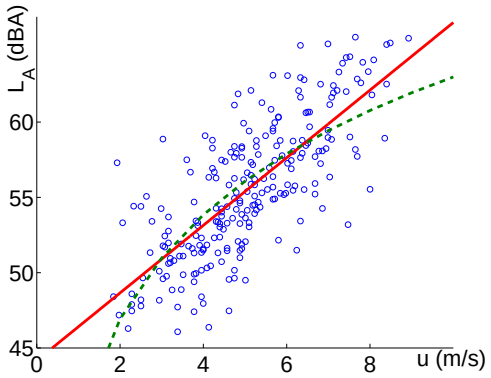

(a) Site 1, (—)$L_A \propto 2.2U$, (- - -)$L_A \propto 23log(U)$

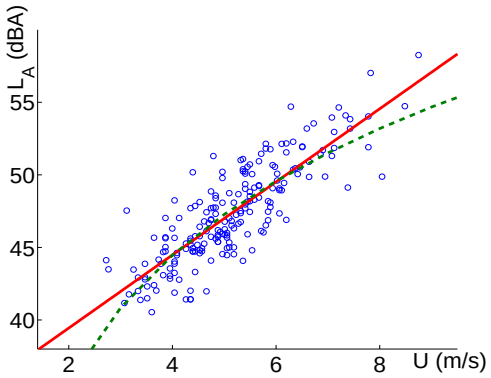

(b) Site 2, (—) $L_A \propto 2.5u$, (- - -) $L_A \propto 29log(U)$

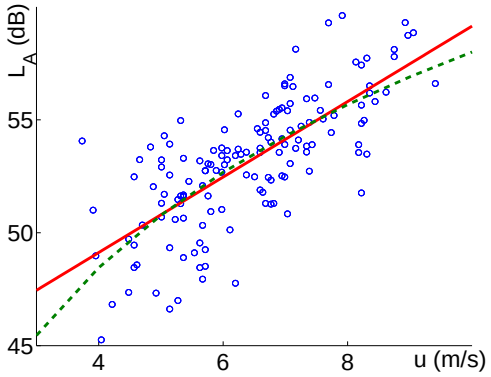

(c) Site 3 Microphone 1, (—) $L_A \propto 1.7U$, (- - -)$L_A \propto 24log(U)$

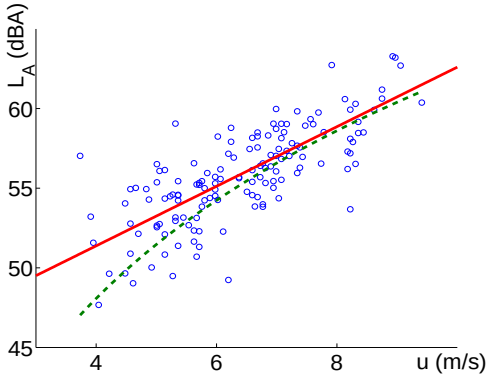

(d) Site 3 Microphone 2, (—) $L_A \propto 2.3U$, (- - -) $L_A \propto 35log(U)$

Figure 15: A-weighed sound pressure levels as a function of wind speed. The line — shows linear least squares approximations and the line - - - line represent logarithmic least squares approximations of the measurement data ○.

levels showed in Figure 15 that deviates most from the linear assessments are removed to disregard from external noise. Average values of sound pressure levels are calculated for each integer value of wind speed, these are plotted in Figure 16. This averaging is performed in order to promote every wind speed equally compared to the former approximation that give equal importance to every measurement point. In this paper the Fégeant approach is considered appropriate due to the fact that the natural boundary condition in equation (14) is satisfied and also because wind tunnel measurements have been used to verify that model.

Concerning the vegetation noise wind speed dependence in the deleafed case a theoretical derivation of the value is presented in this article. Measurements at sites 4 and 5 resulted in very low sound levels at low wind speeds, thereby at

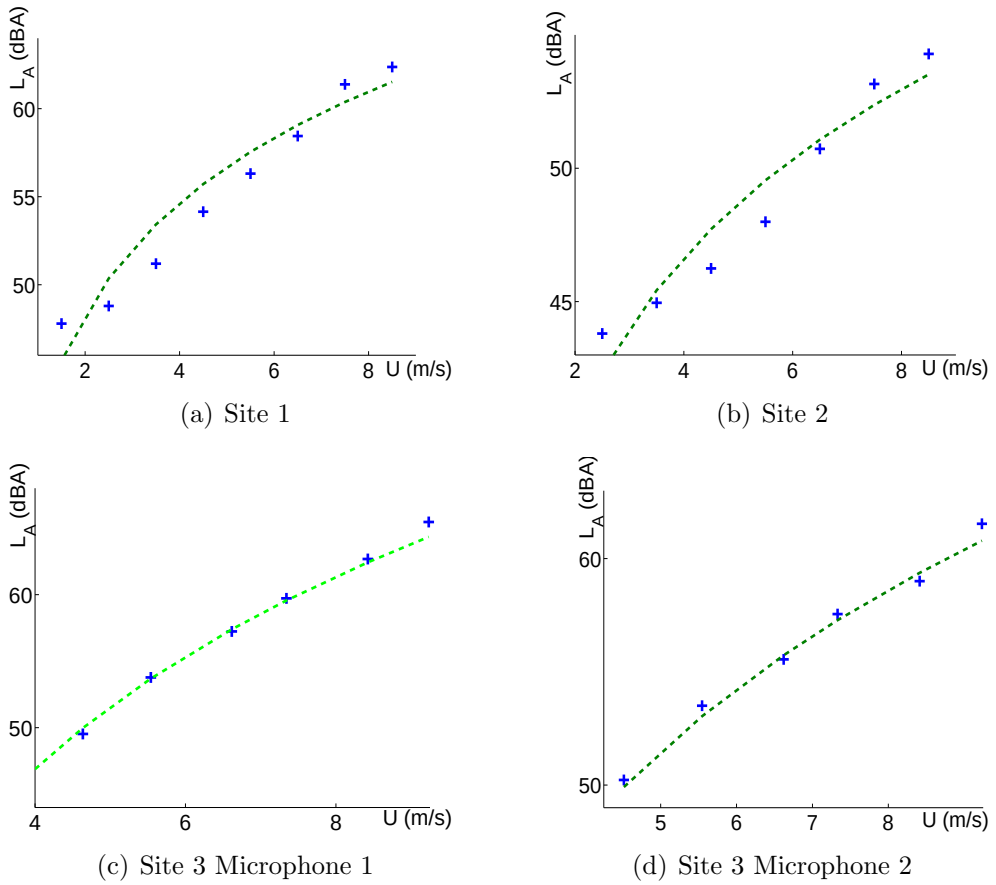

(a) Site 1 (b) Site 2

(c) Site 3 Microphone 1 (d) Site 3 Microphone 2

Figure 16: A-weighed sound pressure levels as a function of wind speed. Average values are marked with a + sign. The line - - - shows predictions from simulations.

these speeds the ambient noise level mask deleafed tree noise and consequently the estimation procedure as in Figure 15 could not be implemented in these measurements. This supports the theory of a high value of χ in equation (12) like dipole sources that have a χ value of 3 ($W \propto M^{2\chi}$). The high porosity expected in the deleafed tree case should contribute to smaller decrease of wind speed compared to trees with full foliage. The theoretical value of $\chi = 3$ seems to give good agreement at the two wind speeds reported but further validation of this parameter could be necessary.

4 Discussion

The objectives of this paper is to evaluate the characteristics of vegetation noise. The developed model is compared to an earlier prediction method and indicate that improved spectral resemblance between predictions and measurements, par-

ticularly in the low frequency region, can be observed. The deviations still present in the low frequency region between the measurements and predictions could mainly be explained by vegetation sources at longer distances not considered, other sources of ambient noise or by the pseudo-noise caused by airflow on the microphone membrane. The model that is proposed in the paper concerning the deleafed trees is the first, to the author's knowledge, of its kind and should give a possibility to predict vegetation noise from deciduous trees with respect to their annual changes, although intermediate states have not been investigated and hence the transition may not be as assumed. The peak in the deleafed spectrum explained by sound generated from the flow around canopy elements is less pronounced in the fully leafed case because of the lower porosity reduce the wind speed inside the foliage. However, the sound emission from the deleafed state has been verified at only two locations. Therefore caution and further measurements are needed in order to adjust the parameters of this model.

The physical mechanisms generating sound in trees are considered to be varying origins in the cases of leafed, deleafed deciduous and coniferous trees. In the fully leafed case the sound generated by the colliding leaves could be modeled as flow acoustic monopoles, similar to sound from clapping hands. Another possible source could be the flow separation around the stalks that should be a dipole source but as no Strouhal frequency can be observed in the measurements this source is probably masked by other sources. It is considered probable that the dominant generation of sound from leafs is explained by the structural borne vibrations caused by collisions in the foliage. The relatively high stiffness and low weight of leafs should produce these surface borne vibrations quite effectively. This hypothesis suggest that dried leaves, occurring in autumn and also in the laboratory measurements by Fégeant, could alter the spectrum as the leafs are both stiffer and lighter; properties that should generate higher frequencies compared to leafs filled with moisture. Another possible sound generating mechanism could be the mechanical vibrations induced by collisions of the canopy elements. The single sound generating mechanism of coniferous trees proposed by Fégeant is questionable as the measured spectrum show low frequency components that could not be explained by flow separation around needles. The low frequency parts of the spectrum could instead be explained by friction-induced sound when canopy elements move and collide with each other and by flow separation around branches and twigs. Similar to coniferous trees the sound generated from trees without foliage should consist of dipole sources. The very high porosity of these canopies should yield a minimum amount of motion in the canopies, thereby other sound sources, such as mechanical vibrations from colliding twigs, in this case should be neglected.

Although a scaling law derived from theoretical assumptions would be very elegant and possibly allow for extrapolating for example wind speed dependence of vegetation noise, this could unfortunately not be achieved. The immense

physical complexity and number of parameters that seems to govern the noise emission from vegetation are prohibiting such method to be presented in this article. Thereby the parametric model proposed above which is shown valid in the measured conditions are considered a sufficient and effective technique to estimate sound from vegetation.

5 Acknowledgment

The author wishes to thank Professor Mats Åbom for helpful discussions and is also grateful to PhD Susann Boij for proofreading. This study was supported by the Swedish wind energy foundation VINDFORSK research grant number 20134-2.

References

[1] O Fégeant. Wind-induced vegetation noise. part 1: A prediction model. *Acta Acustica*, 85:228–240, 1999.

[2] O Fégeant. Wind-induced vegetation noise. part 2: Field measurements. *Acta Acustica*, 85:241–249, 1999.

[3] O Fégeant. Masking of wind turbine noise: Influence of wind turbulence on ambient noise fluctuations. Technical Report 2002:12, Department of Civil and Architectural Engineering, Royal Institute of Technology, Sweden, 2002.

[4] International Organization for Standardization, Geneva, Switzerland. *ISO/DIS 9613-1: Attenuation of sound during propagation outdoors- Part 1: Atmospheric absorbtion*, 1995.

[5] M E Delany and E N Bazley. Acoustical properties of fibrous absorbent materials. *Applied Acoustics*, 3:105–116, 1970.

[6] J Kragh et al. Nordic environmental noise prediction methods. nord2000. Technical Report 1719/01, Delta Acoustics, Lyngby, 2001.

[7] J J Landsberg and G James. Wind profiles in plant canopies: Studies on an analytical model. *J. Appl. Ecology*, 8:729–741, 1971.

[8] R Milne. *Wind and trees, M P Coutts and J Grace*, chapter Modelling mechanical stresses in living stika spruce stems, pages 165–181. Camebridge University press, 1995.

[9] J D Lin Z Li and D R Miller. Air flow over and through a forest edge: a steady-state numerical simulation. *Boundary layer meteorology*, 51:179–197, 1990.

[10] O Fégeant. Wind turbine noise assessment. Technical report, Building Acoustics, KTH, Stockholm, 1997. TRITA-BYT 1997-175.

[11] International Organization for Standardization, Geneva, Switzerland. *ISO/DIS 1996: Acoustics- Description and measurement of environmental noise*, 1986.

[12] Federal Ministry for Environment, Nature Conservation and Nuclear Safety, Bundesministerium für Umwelt, Naturschutz und Reaktorsicherheit. *TA-Luft, Erste Allgemeine Verwaltungsvorschrift zum Bundes-Immissionsschutzgesetzt- Techniche Anleitung zur Reinhaltung der Luft (First general directive to the federal immission protection act- Technical guideline for clean air)*, 2002. (in German).

[13] D Miller. The two dimensional energy budget of a forest edge with field measurement of a forest parking lot interface. *Agricultural Meteorology*, 22:53–78, 1980.

[14] M Sneddon et al. Measurements and analysis of the indigenous sound environment of coniferous forests. Technical report, BBN System and Technologies, 1994. NPOA Report No. 91-1, BBN Report No.7210.

Influence of turbulence and wind speed profiles on vegetation noise

Karl Bolin
Royal Institute of Technology / Marcus Wallenberg Laboratory
Teknikringen 8
SE-100 44 Stockholm
Sweden
+46-(0)8 790 92 02
kbolin@kth.se

Abstract

Different wind models have been investigated and implemented in the vegetation noise model from paper A. It is shown that atmospheric conditions could have a strong influence on both the sound pressure level, due to changing vertical velocity profiles, and the sounds temporal fluctuations caused by changing amounts of wind turbulence. Simulations of time fluctuating vegetation noise show good agreement compared with experimental data from three different sites.

1 Introduction

In several countries the wind turbine noise issue is becoming an accentuated problem as the demand for renewable power sources are accelerating when signing states of the Kyoto protocol are obliged to fulfill their reduction of green-house gases. The noise emission limits for wind turbine noise differ from country to country. The Dutch emission limits [1] are coupled to the wind speed at 10 m height, thereby implicitly taking the background noise level into account. In the article by v.d. Berg [2] measurements showed differences of 15 dBA on wind turbine noise at the same wind speed at 10 m height but in different vertical velocity profiles. Thereby questioning the validity of the Dutch approach and emphasizing the need to accurately model the wind, when investigating noise sources generated by the wind. In Britain the noise legislation [3] correlates the emission

limits to measured ambient noise levels correlated to the wind speed. This procedure allows for optimum noise emission without causing annoyance at nearby dwellings, but is time consuming and expensive as measurements should be performed at all seasons and different meteorological conditions for determination of correct noise limits, also changing vertical velocity profiles are not accounted for. In the case when vegetation noise is dominant the measurements could be replaced by the prediction methods proposed by Fégeant in [4] and [5] or by Bolin in paper A [6]. These models correlate the emitted sound from vegetation to the average wind velocity, thereby predicting the background noise without extensive measurements. However the wind turbulence, discussed in [7], and the changes in wind dynamics caused by different atmospheric conditions could possibly alter the emitted sound and are therefore investigated in this paper. This article present turbulence models and vertical wind speed profiles depending on the atmospheric conditions coupled to the vegetation noise model in paper A [6]. Furthermore measurements of the vegetation noise dependence on turbulence and comparison with the simulation results are presented. This article can therefore be used to evaluate the masking potential by vegetation noise on for example wind turbine noise when reasonably advanced meteorological models are taken into account.

2 Wind models

2.1 Average wind

The mean wind speed is defined in general as the wind velocity over ten minute intervals [8]. The average wind direction is denoted x and the mean wind speed U, see Figure 1. The average wind spatial characteristics change in foliage compared to in open terrain, these changes are described below.

2.1.1 Flow inside forests

Wind velocity models of flow in and around vegetation have received considerable attention in the field of boundary layer meteorological research. Among others Panovsky and Dutton [9] and Kaimal and Finnigan [10] wrote excellent books on the subject and explained flow inside tree canopies. In the paper of Cionco [11] the vertical velocity profile in an infinite forest is expressed as

$$U(z) = U_H e^{a(z/H-1)} \tag{1}$$

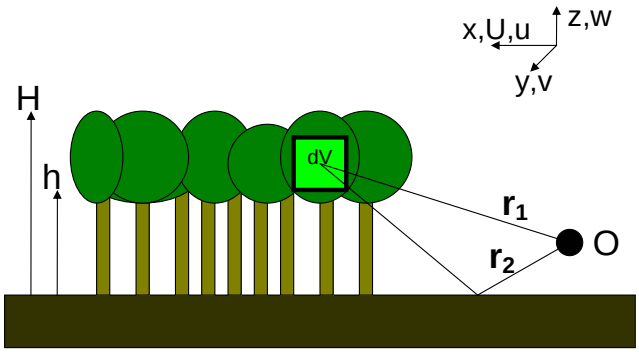

Figure 1: Geometry of vegetation with tree height H, trunk free height h, volume element dV, propagation paths $\mathbf{r_1}$ and $\mathbf{r_2}$ to observer position $\mathbf{O}$. In the upper right corner the Cartesian coordinates $(\mathbf{x}, \mathbf{y}, \mathbf{z})$ where $\mathbf{x}$ corresponds to the mean wind direction with wind speed $\mathbf{U}$ and turbulence u, $\mathbf{y}$ is the horizontal direction prependicular to $\mathbf{x}$ and $\mathbf{z}$ is the vertical directions with their respective wind components v and w.

where U_H is the wind speed at the height H. This wind speed profile is also valid in a upwind forest edge [4] as the wind profile will propagate unaltered in the forest untill the forest edge is reached.

2.1.2 Flow in open terrain

In the case of downwind forest edges and single trees, the vertical velocity profile of the free field is propagating a distance of approximately $2H$ inside the canopies according to smoke visualizations performed by Miller [12]. Therefore an edge region with a velocity profile from the open terrain can be expected in this volume.

In the paper by van den Berg [2] the emission of wind turbine noise is correlated to the changing of wind profile with respect to atmospheric conditions. Therefore it is considered of interest to examine the effect on sound from vegetation at different atmospheric conditions as this effect has not been taken into account in earlier models. Atmospheric conditions are usually separated into stable, neutral and convective conditions. A stable atmosphere occur when the temperature gradient $dT(z)/dz = \theta(z) > \theta_{adiabatic} = 0.0066°\text{C/m}$ and thus the air at lower heights has higher density than the air above therefore reducing the vertical wind motion. This condition occur for example on clear nights when the ground is colder than the air and results in large variations of wind speed with respect to height. A neutral atmosphere is characterized by a temperature gradient $\theta(z) \approx \theta_{adiabatic}$ and is often used as a reference case as it is the intermediate state between the other two conditions. The convective or unstable condition occurs when $\theta(z) < \theta_{adiabatic}$, present for instance on warm sunny days as the

heated ground causes high amounts of vertical wind motions and turbulence, this mixing of air results in wind speeds that is changing less with respect to height. The vertical velocity profile is thus depending on the atmospheric conditions and this is modeled by The German Air Quality Guideline "TA-Luft" [13] by

$$U(z) = U_{ref}\left(\frac{z}{z_{ref}}\right)^m \tag{2}$$

where U_{ref} is the mean wind velocity at the height z_{ref} and m varies according to table 1.

Atmospheric condition	m
Very unstable	0.09
Moderately unstable	0.20
Neutral	0.22
Slightly stable	0.28
Moderately stable	0.37
Very stable	0.41

Table 1: Velocity profile parameter m for different atmospheric conditions.

To illustrate the results of changing atmospheric conditions, an example with the velocity profiles of the two extreme values of m in table 1 are shown below. The normalized wind speed at $z = 10\,m$ height is shown in Figure 2(a). Although the integral

$$\int_{z=0}^{20} U(z)dz \tag{3}$$

vary less than 4% between the two extreme conditions for the same wind speed at the reference height z=10 m the resulting change in sound pressure level Figure 2(b) is about 3 dB for an edge of aspens with trunk height of 8 m, tree height of 17 m and at a wind speed of 2.5 m/s at the reference height z=10 m. Hence it is concluded that different atmospheric conditions might have significant impact on the vegetation noise levels.

2.1.3 Attenuation in forest edges and compact vegetation sources

When the wind propagate from open terrain into vegetation the wind speed is reduced, this attenuation depend on the porosity ϕ normally around 50% for vegeation sources it is also depending on the horizontal attenuation coefficient ϑ=0.08 for foilages with average leaf area density S according to equation (4)

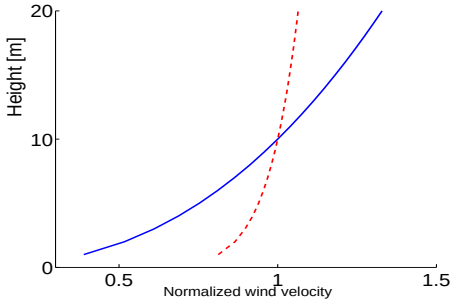

(a) Wind velocity profile $0 < z < 20\,m$ normalised with respect to $U(z = 10\,m)$.

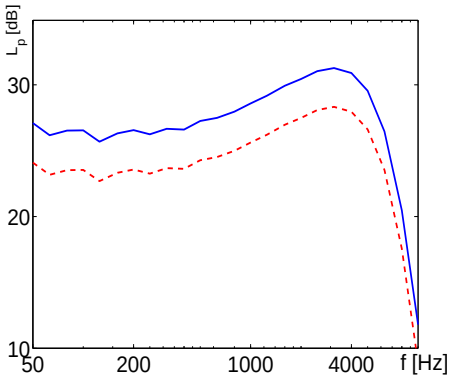

(b) Third octave band sound pressure levels for downwind forest edge of aspens at a wind speed of $2.5\,m/s$.

Figure 2: Vertical wind speed profile and simulated sound pressure level for very stable (—) respectively very unstable (- - -) atmospheric conditions.

$$\frac{U(d)}{U_0} = \sqrt{\phi} e^{-\vartheta\, S\, d} \tag{4}$$

where U_0 is the wind speed at the forest edge and d is the distance to the forest edge in the average wind direction.

2.2 Wind Turbulence

In this section the temporal variations of wind speed, known as turbulence [8], is investigated. Wind turbulence in and around vegetation has been attracting attention from several researchers (see [14], [15] and [16]). The statistical properties assigned to turbulence in a complex terrain differ from that of flat and smooth surfaces. The turbulence effect on vegetation noise are examined in the report [7]. However, the proposed turbulence model is not valid for arbitrary vegetation types but only for those with small extension and a one dimensional turbulence model is used, neglecting turbulence perpendicular to the mean wind direction. Therefore it is considered of interest to investigate if turbulence models coupled to a vegetation noise generation model are able to predict the temporal variations of vegetation noise and also if a three dimensional model changes the temporal variations in vegetation noise compared to a one dimensional model.

In [7], Fégeant derived a theoretic probability density function of sound pressure levels in small vegetation geometries. The standard deviation σ of the sound pressure level L_p is there estimated by

$$\sigma_{Lp} = \frac{20 \cdot 2\chi}{ln(10)} \cdot i_u \tag{5}$$

where χ is the wind speed coefficient see paper A [6] and i_u is the wind turbulence intensity in the mean wind direction. The work in [7], although innovative, contained assumptions of moderate turbulence intensities, $i_u = \sigma_u/U$, $i_v << i_u$ and $i_w << i_u$, conditions that are considered fulfilled in open terrain, however not inside forests. These assumptions can indeed be considered valid in stable and neutral atmospheric conditions, but as shown by Andrén [17] the turbulence intensities at unstable atmospheric conditions are much higher than in the other two cases. Furthermore, the assumption of an open terrain [18] might be invalid in most applied locations as trees or other obstacles upwind may disturb the flow and thereby causing increased turbulence intensities.

2.2.1 Atmospheric conditions

Not only the vertical velocity profile changes in different meteorological conditions but also the turbulence intensities vary markedly, see [17]. The article uses measurements of wind speed standard deviation, σ, from several different locations and at different atmospheric conditions. A stable atmosphere can be estimated by equation (6)

$$\frac{\sigma_u^2}{U_*^2} = 3.0 \tag{6}$$

where $U_* = 0.237$ (m/s) is the reported friction velocity from that measurement location. At the same site the horizontal variance perpendicular to the mean wind direction is expressed by equation (7)

$$\frac{\sigma_v^2}{U_*^2} = 1.5 \tag{7}$$

In another measurement location the neutral atmosphere the variance in the surface layer is approximated by

$$\frac{\sigma_u^2}{U_*^2} = 2.9 \tag{8}$$

with a friction velociy $U_* = 0.388$ (m/s).

The measurements differed at this site comared to the first location in the unstable or convective case where the total velocity variances were measured instead by

$$\frac{\sigma_u^2 + \sigma_v^2}{2w_*^2} = 0.274 \tag{9}$$

where a different normalization parameter, the convective velocity scale $w_* = 1.44$ (m/s) is used. Combining equation (6) and (7) yields that the variance perpendicular to the mean wind direction are expressed as

$$\sigma_v^2 = 1.5U_*^2 = \frac{\sigma_u^2}{2} \tag{10}$$

In this paper the relative ratios of the turbulence intensities are assumed constant at different atmospheric conditions. Consequently the equations (9) and (10) are combined to give the variance in the mean wind direction at unstable conditions as

$$\frac{\sigma_u^2 + \sigma_v^2}{2w_*^2} = \frac{3\sigma_u^2}{4w_*^2} \Rightarrow \frac{\sigma_u^2}{w_*^2} = \frac{4}{3} \cdot 0.274 \tag{11}$$

From equations (6), (8) and (11) it can be noted that the magnitude of the variances in the mean wind direction are

$$\sigma_{neutral}^2 = 0.60\, \sigma_{unstable}^2 = 2.65\, \sigma_{stable}^2 \tag{12}$$

concluding that turbulence intensities varies not only with different surface structures but also with different atmospheric conditions. This should affect the variations of vegetation noise.

2.2.2 Time series of space- and time-correlated wind speeds

The non-deterministic nature of wind turbulence can be modeled as a stochastic process correlated in space and time. In order to extract time series of wind velocities the Sandia method [19] have been developed to estimate wind fluctuations around wind turbine sites, but is here being used for larger areas to simulate the wind field in the vegetation. The interesting area to simulate wind series in [19] and [20] is two dimensional, in the vegetation source application this should be extended to three dimensions which result in a large number of computations

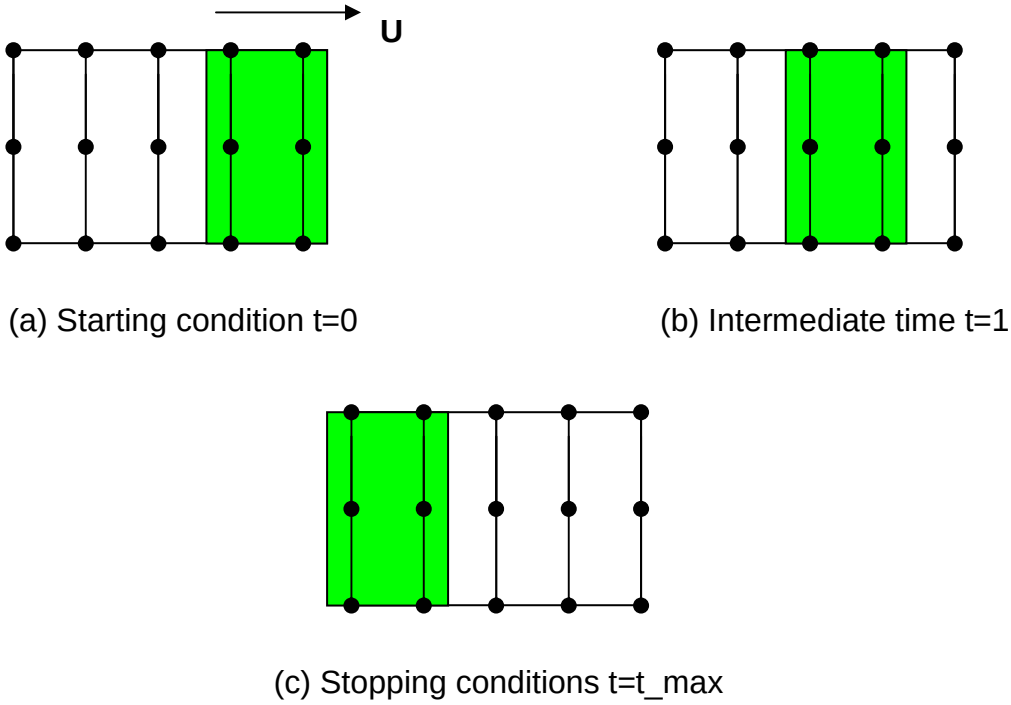

Figure 3: Wind speeds are calculated for every point (•) in the discretisized plane, the vegetation is in the shaded area. The wind speed simulation is then starting as shown in (a) and then this mesh is then propagated in the **U** direction as shown in (b) to the final state (c).

needed to acquire turbulent wind speeds of statistically significant length. To decrease the number of computations a two dimensional plane at a reference height of 10 m is constructed and wind speeds are computed for this instead of a fully three dimensional space. The wind speed profiles in equation (1) and equation (2) are then used to extrapolate wind speeds in the vertical direction. In order to reduce the number of computations further in the Sandia method "Taylor's frozen eddy" hypothesis [8] is assumed valid. This theory assumes that turbulence velocities are unchanged but propagate a vector $\mathbf{L} = \mathbf{U}\Delta t$ during the time Δt. The Sandia method create a mesh of space and time correlated wind speeds at different discrete points in the plane as seen in Figure 3. After the mesh has been calculated it can be propagated over the discretisized region containing vegetation. If the vegetation is a downwind forest edge or a compact source the wind speeds are corrected with respect to the horizontal attenuation in equation (4).

The Sandia methods mathematical algorithm are described below, for more details see [19]:

1. **Cross spectrum, C**

   The diagonal elements in the cross spectrum matrices in point l and fre-

quency f_l are defined by

$$c_{ll}(f_l) = \frac{\Delta f_l}{2} S_l(f_l), \quad l = 1, 2, ..., M \tag{13}$$

where $S_l(f_l)$ is the power spectrum density. This function describes the correlation of the wind speed in the frequency domain. It is essential that power spectral densities adjusted to complex terrain is used in order to obtain correct temporal fluctuations of the wind. Standard spectra in use are the von Karman and the Kaimal spectrum but these are valid only under certain conditions.

Tieleman presents a three dimensional model in the paper [18] adapted to complex terrain and neutral atmospheric conditions described for all three directions which estimate the power spectral densities $S_n(f_l)$ normalized by the variance in the different directions $\sigma^2_{Su,Sv,Sw}/U^* = 6.25$, 4 and 1.56 for the components u, v and w.

$$\begin{aligned} \frac{S_u(f_l)}{\sigma^2_{Su}} &= \frac{40.42U/z}{(1 + 60.62f_l)^{5/3}} \\ \frac{S_v(f_l)}{\sigma^2_{Sv}} &= \frac{13.44U/z}{(1 + 20.16f_l)^{5/3}} \\ \frac{S_w(f_l)}{\sigma^2_{Sw}} &= \frac{3.28U/z}{(1 + 4.92f_l)^{5/3}} \end{aligned} \tag{14}$$

where f_l is the wind frequency, the necessary frequency resolution $\Delta f = 1/T$ are depending on the total simulated time T or t_{max} this was set to 300 s in the simulations presented later in this paper. Power spectral densities are thus calculated in the frequency interval between $[\Delta f, 1]$ (Hz). The friction velocity U_* can be calculated by

$$U_* = \frac{0.4U}{log(z/z_0)} \tag{15}$$

where z_0 is the roughness length estimated to 0.5 m in complex terrain [8]. Comparisons between the spectra of Kaimal and Tieleman are shown in Figure 4.

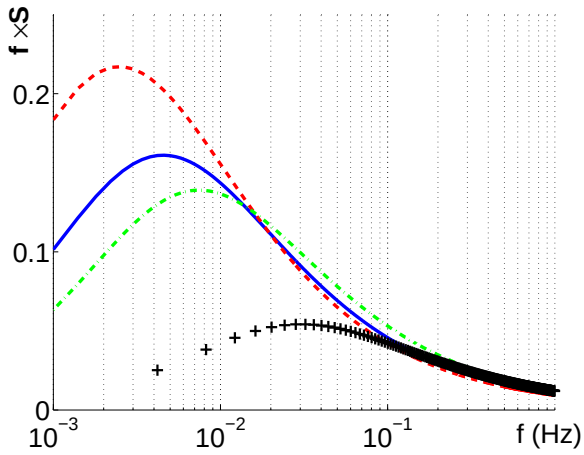

Figure 4: Power Spectrum Density of Kaimal (—) and Tieleman (- - -), (-.-) and (+) for the (u,v,w) components shows that the peak frequency is lower in the PSD in the mean wind direction this results in time series with stronger low frequency fluctuations.

The non diagonal elements of the cross spectrum matrices are also depending on the coherence function $Coh(f_l, \Delta r_{lk}, u)$ between different points d and k, this is calculated by equation (16)

$$|c_{dk}(f_l)| = Coh(f_l, \Delta r_{dk}, u)\sqrt{c_{dd}c_{kk}} \tag{16}$$

By assuming that there is an average phase of zero [20] between points d and k the cross spectra is defined by S and the coherence function that is expressed as equation (17)

$$Coh(f_l, \Delta r_{dk}, u) = e^{\frac{-L\Delta r_{dk} f_l}{U}} \tag{17}$$

where r_{dk} is the distance between the points d and k, u is the average wind speed, $L = 7.5$ is a constant according to Veers [20].

2. **Choleskey decompositioning**

   Each cross spectrum matrix is Choleskey decompositioned according to

$$\mathbf{C}(f_l) = \mathbf{H}\mathbf{H}^T \tag{18}$$

   where $\mathbf{H}$ is an under triangular matrix.

3. **Random matrix**

To simulate the non deterministic characteristics of turbulent flow a vector of length M with random entries is created. This is generated for each frequency component, l, according to

$$x_{dl} = e^{j2\pi\beta_{dl}} \tag{19}$$

where d is index of the elements, l is the number of the frequency and β_{dl} is a normalized random variable uniformly distributed over the interval $[0, 1]$.

4. **Time series of turbulent flow**

   In order to transform the results from frequency domain to time domain

$$\mathbf{V} = \mathbf{HX} \tag{20}$$

   is calculated, $\mathbf{V}$ is the Fourier coefficients for a time series representing wind turbulence. Hence the time series are computed for every discrete point in the mesh by an inverse fast Fourier transform.

$$\mathbf{U}(t) = FFT^{-1}(\mathbf{V}) \tag{21}$$

It is assumed in this paper that the wind turbulence in different directions are independent of each other therefore the directions can be simulated separately. Thereby this algorithm is implemented for the $\mathbf{x}-$, $\mathbf{y}-$ and $\mathbf{z}-$ direction generating $u(t)$, $v(t)$ and $w(t)$ as independent time series of wind turbulence. In order to compensate for different atmospheric conditions from section 2.2.1 these time series which are valid for a neutral atmosphere are multiplied by scaling factors from equation (12) which result in the following expression

$$\begin{aligned} (u,\, v,\, w)_{stable} &= (u,\, v,\, w)_{neutral} \cdot\ 2.65^{-1/2} \\ (u,\, v,\, w)_{unstable} &= (u,\, v,\, w)_{neutral} \cdot 0.60^{-1/2} \end{aligned} \tag{22}$$

which should get the time series adjusted to different atmospheric conditions.

If a three dimensional wind speed simulation of the Sandia method are performed the wind speed $U_{tot}(t)$ can be computed by combining the mean wind speed, U, with the turbulent time series according to

$$U_{tot}(t) = \sqrt{(U + u(t))^2 + v(t)^2 + w(t)^2} \tag{23}$$

In the case of only turbulence in the mean wind direction is evaluated the expression (23) reduces to

$$U_{tot}(t) = U + u(t) \tag{24}$$

2.2.3 Calculation of time fluctuating vegetation noise

The wind speeds, generated by the Sandia method, are inserted as input into the discrete vegetation noise model presented in paper A [6] and the generated sound power from each discrete point is estimated. To reduce the number of calculations the vegetation noise model calculate the sound emitted at discrete wind speeds from 0 m/s up to 30 m/s and these values are tabled for every discrete vegetation area. The wind speeds are then rounded to the nearest integer value and the sound power from the noise model are estimated for every time step. The algorithm are sketched in Figure 5.

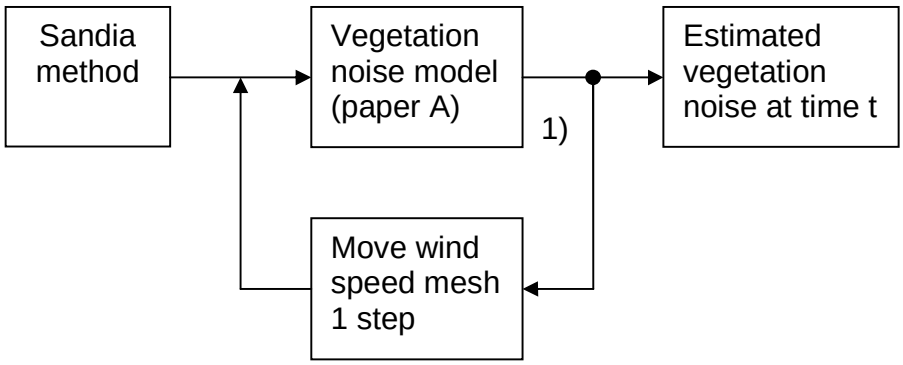

Figure 5: Calculation procedure to estimate time fluctuating vegetation noise.

3 Measurements

To investigate the temporal fluctuations of vegetation noise a new set of measurements were performed. Earlier, two measurements of time varying vegetation noise have been performed in [7], however the first measurement was performed close to a shelterbelt of elms a tree species not investigated in any known noise model. At a second site, consisting of aspen, spruce and pine trees, the exact

vegetation geometry and meteorological data were not reported. Therefore new measurements were considered necessary in order to clarify the temporal variations of vegetation noise. Measurements have been performed at three different locations, these are described in detail in paper A [6] and are referred to as site 1, 2 and 3. Unfortunately no temperature gradients were possible to measure due to lack of equipment, however by observing the weather it is considered that this can be estimated with sufficient accuracy. The measurements at site 1 and 2 were performed in November, the low intensity of the solar radiation combined with strong winds and cloudy weather suggest that the atmospheric conditions should be neutral [8]. At site 3 measurements took place in September the atmospheric condition is assumed unstable due to the relative high amount of solar radiation which should cause convection of the air closest to the ground.

3.1 Turbulence and fluctuations of sound levels

Statistic properties of A-weighed sound pressure level and wind speed are shown in table 2. In order to reduce the influence of pseudo-noise, the sound levels are A-weighed as this procedure reduce low frequencies. Even though the foam windscreen reduces the pseudo-noise this still sometimes dominates the recorded periods, these time sequences are manually removed from the analyzed data.

		Measurement		**3D Simulation**		**1D Simulation**	
		U (m/s)	L_A (dBA)	U (m/s)	L_A (dBA)	U (m/s)	L_A (dBA)
Site 1	$\bar{x}$	5.1	55.2	5.2	54.1	5.1	51.8
	σ_x	1.7	4.0	1.8	2.8	2.0	2.9
Site 2	$\bar{x}$	6.3	47.2	6.3	50.9	6.3	48.0
	σ_x	1.5	3.0	1.6	3.4	1.1	3.1
Site 3 Mic 1	$\bar{x}$	5.2	56.8	5.2	56.2	5.1	56.0
	σ_x	1.7	2.6	1.5	2.6	1.5	2.7
Site 3 Mic 2	$\bar{x}$	5.2	59.5	5.2	56.9	5.1	56.7
	σ_x	1.7	5.2	1.8	2.8	1.8	2.8

Table 2: Measured wind speed and sound levels, $\bar{x}$ denote average values and σ_x standard deviation.

If the measurements are compared to their respective simulations in table 2 it can be observed that the sound levels agree well at site 1 and site 3 microphone 1. The differences at site 2 might be explained by misjudgment of the vegetation's extension and at site 3 microphone 2 by that the shrubberies under the

vegetation is not included in the simulation. The wind´s standard deviation are well estimated by both three and one dimensional simulations and it is therefore concluded that the one dimensional turbulence model is sufficiently accurate. Thereby the assumptions that (i) the relative ratios of the turbulence intensities are assumed constant at different atmospheric conditions and (ii) the wind turbulence in different directions are independent of each other are not necessary as wind turbulence perpendicular to the mean wind direction have only a marginal effect on the time fluctuations of vegetation noise. The compact vegetation source theoretical standard deviation of sound pressure level σ_{Lp}, equation (5) proposed in [7] is computed for the second location, the only measurement from a compact source and gives an estimated standard deviation of 6.2 dBA. This clearly overestimates the standard deviation of vegetation noise as can be seen in Figure 2, therefore this expression could be considered an inaccurate method of estimating sound fluctuations of vegetation noise.

3.2 Distribution

Measured cumulative distributions of 1 s A-weighed sound pressure levels are shown in figures 6-9. Fégeant [7] showed that large vegetation sources could be viewed as having normal distributions of sound pressure level but simulations compared to these measurements were not performed. As shown the sound pressure levels cumulative distributions are almost completely Gaussian in the intervals between 10% and 90%. The linear regression lines for measurements and simulations shows large similarities. The steps observed in simulation results see Figures Figures 6(b) and 7(b) are due to a computaional algotithm were wind speeds at the discrete points are rounded to the nearest integer. This procedure is adopted to decrease the number of computations needed and have smaller effect when large regions are simulated see Figures 8(b) and 9(b). Deviations from Gaussian distribution in simulated time series could depend on the relatively short simulated time (300 s) compared to measured time series (1200 s).

The normal distributions shown as dotted lines in Figures 6-9 have steeper slopes in the measurements compared to the simulations. This should be interpreted as that the variations are underestimated in the simulations. The reason for this might be either that the estimations of atmospheric conditions were wrong or that the spatial coherence in equation (17) are less at these locations compared to the paper [18].

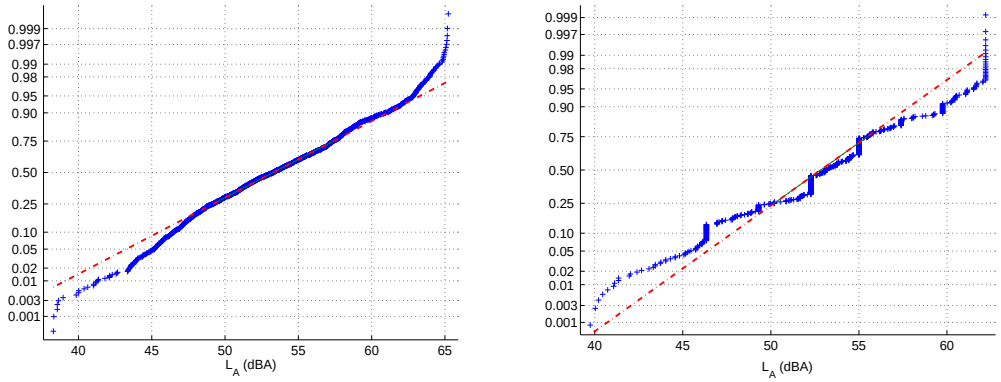

(a) Measurement (b) Simulation

Figure 6: Cumulative distribution of A-weighed sound pressure level at site 1. Data points are shown as + and linear approximations as - · -

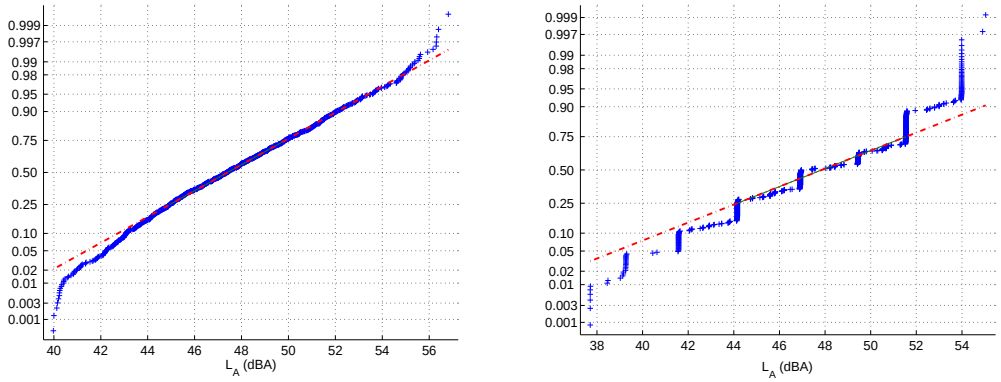

(a) Measurement (b) Simulation

Figure 7: Cumulative distribution of A-weighed sound pressure level at site 2. Data points are shown as + and linear approximations as - · -

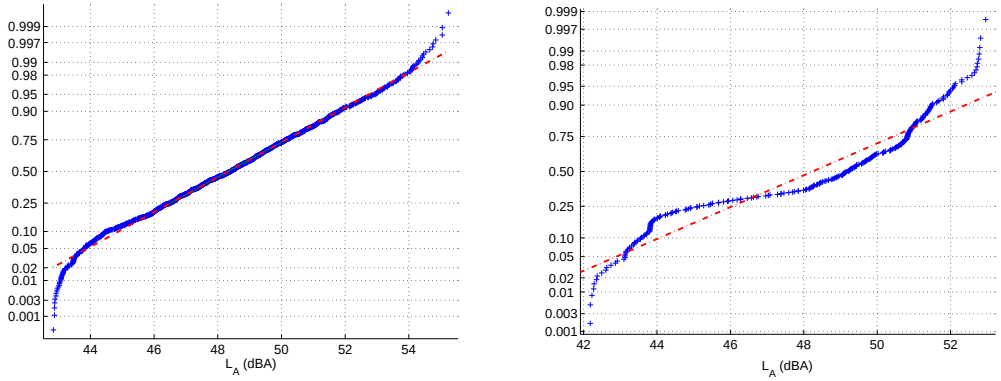

(a) Measurement (b) Simulation

Figure 8: Cumulative distribution of A-weighed sound pressure level at site 3, microphone 1. Data points are shown as + and linear approximations as - · -

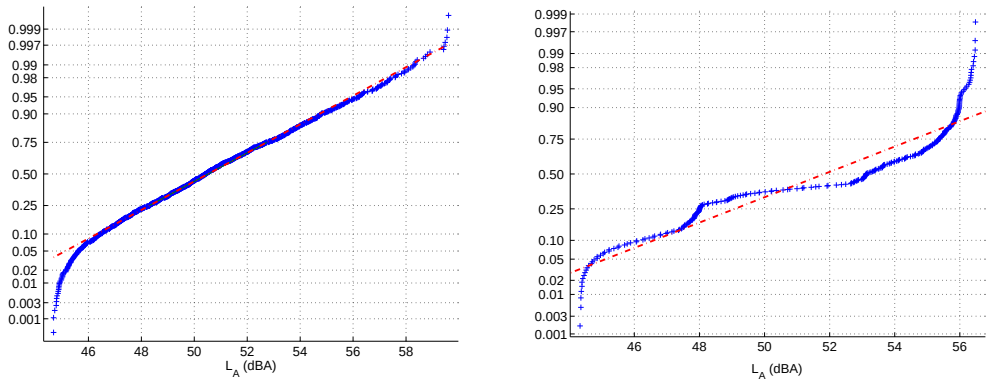

(a) Measurement

(b) Simulation

Figure 9: Cumulative distribution of A-weighed sound pressure level at site 3, microphone 2. Data points are shown as + and linear approximations as - · -

4 Conclusion

Steady and turbulent wind models have been examined and the implications of changing atmospheric conditions have been evaluated, this changes the turbulence intensities and the vertical velocity profile considerably thereby resulting in large deviations from the neutral atmosphere which were used as the default condition in earlier prediction methods, [4], [5]. It has been shown that both measurements and simulations of time varying vegetation noise can be approximated by Gaussian distributions for both small and large vegetation sources. Unfortunately no long time measurements have been performed that could verify the simulated variations due to changing wind speed profiles. However the straightforward connection between wind speed and vegetation noise leads to the conclusion that, although not measured, the vertical wind speed profile will have a large impact on the sound generated from vegetation.

The applications of this article is to enable assessment of the masking potential of vegetation noise on wind turbine noise with higher accuracy compared to if turbulence and varying velocity profiles are neglected. The procedure of modeling background noise compared to measuring it has two main advantages. Firstly measurements should be performed at all seasons to account for changing environmental conditions, leafed or deleafed trees etc. Unnecessary to mention these measurements will be both time consuming and costly compared to measurements. Secondly the existence of other disturbing noise sources such as traffic noise and aircraft noise should not allow for higher noise limits from wind turbines, if these not completely mask the wind turbine noise, otherwise the wind turbine noise will add menace to an already polluted environment. This risk can elegantly avoided by simulating vegetation noise instead of measuring it.

5 Acknowledgment

The author wishes to thank Professor Mats Åbom for helpful discussions. This study was supported by the Swedish wind energy foundation (VINDFORSK) research grant number 20134-2.

References

[1] A W Bezemer et al. Handleidingmeten en rekenen industrielawaai (manual for measuringand calculatingindustrial noise). Technical Report 53-86, Den Haag, 1999. (in Dutch).

[2] G P van den Berg. Effects of the wind profile at night on wind turbine sound. *Journal of Sound and Vibration*, 277:955–970, 2004.

[3] R Meir et al. The assessment and rating of noise from wind farms. Technical Report ETSU-R-97, ETSU, Department of Trade and Industry, 1996.

[4] O Fégeant. Wind-induced vegetation noise. part 1: A prediction model. *Acta Acustica*, 85:228–240, 1999.

[5] O Fégeant. Wind-induced vegetation noise. part 2: Field measurements. *Acta Acustica*, 85:241–249, 1999.

[6] K Bolin. Prediction method for vegetation noise. *Paper A*, 2006.

[7] O Fégeant. Masking of wind turbine noise: Influence of wind turbulence on ambient noise fluctuations. Technical Report 2002:12, Department of Civil and Architectural Engineering, Royal Institute of Technology, Sweden, 2002.

[8] J G McGovan J F Manwell and A L Rogers. *Wind Energy Explained*. John Wiley & Sons, New York, 2002.

[9] H Panovsky and J Dutton. *Atmospheric Turbulence*. John Wiley & Sons, New York, 1984.

[10] J C Kaimal and J J Finnigan. *Atmospheric Boundary Layer Flows*. Oxford University Press, New York, 1994.

[11] R C Cionco. A wind profile index for canopy flow. *Boundary Layer Meteorolgy*, 3, 1972.

[12] D Miller. The two dimensional energy budget of a forest edge with field measurement of a forest parking lot interface. *Agricultural Meteorology*, 22:53–78, 1980.

[13] Federal Ministry for Environment, Nature Conservation and Nuclear Safety, Bundesministerium für Umwelt, Naturschutz und Reaktorsicherheit. *TA-Luft, Erste Allgemeine Verwaltungsvorschrift zum Bundes-Immissionsschutzgesetzt- Techniche Anleitung zur Reinhaltung der Luft (First general directive to the federal immission protection act- Technical guideline for clean air)*, 2002. (inGerman).

[14] R Cionco. Intensity of turbulence within canopies with simple and complex roughness elements. *Boundary Layer Meteorology*, 2:453–465, 1972.

[15] D Baldocchi and T Meyers. A spectral and lag-correlation analysis of turbulence in a decideous forest canopy. *Boundary Layer Meteorology*, 45:31–58, 1988.

[16] B Amiro. Comparison of turbulence statistics within three boreal forest canopies. *Boundary Layer Meteorology*, 51:345–364, 1990.

[17] A Andrén. Evaluation of a turbulence closure scheme suitable for air pollution applications. *Journal of Applied Meteorology*, 29:224–239, 1990.

[18] H W Tieleman. Universality of velocity spectra. *Journal of wind engineering and industrial dynamics*, 56:55–69, 1995.

[19] P S Veers. Modeling stochastic wind loads on vertical axis wind turbines. Technical Report SAND83-1909, Sandia National Laboratories, 1984.

[20] P S Veers. Three-dimensional wind simulation. Technical Report SAND88-0152, Sandia National Laboratories, 1988.

Determining the potentiality of masking wind turbine noise using natural ambient noise

Karl Bolin and Shafiquzzaman Khan

Marcus Wallenberg Laboratory, Kungliga Tekniska Högskolan (KTH), Teknikringen 8, SE-100

44 Stockholm, Sweden

Corresponding Address:

Associate Professor Dr. Shafiquzzaman Khan,
KTH – Farkost & Flyg
Teknikringen 8
100 44 Stockholm
Sweden
E-mail: shafik@kth.se
Tel: +46 8 790 8910
Fax: +46 8 790 7629

Summary

The present study investigates the masking potentiality of wind turbine noise in the presence of natural ambient noises, namely vegetations (coniferous and deciduous) and sea wave noises. Thirty six persons performed four different listening tests. Two of the tests were to determine the threshold of wind turbine noise in the presence of the natural ambient noise. The third test was to determine the perceived proportion of wind turbine and natural ambient noise at various S/N ratios (S is wind turbine noise and N is natural ambient noise). The fourth test was to examine the partial loudness of wind turbine noise in the presence of natural ambient noise. The results of the threshold test showed that the average masking threshold S/N ratios varied from -5.3 dBA to -2.6 dBA, where coniferous noise revealed better masking potentiality than the other natural ambient noises (deciduous and sea wave). The S/N ratio test also showed that the potentiality of masking effects of coniferous noise was better at S/N ratio of - 3 dBA than the other natural ambient noises. The S/N ratio test also revealed that the proportion of wind turbine noise was perceived as less than 50% of the total noise at S/N ratio of 3 dBA and below. This S/N ratio of 3 dBA was lower than the British limit of 5 dBA which is used to avoid annoyance from the wind turbine noise. The partial loudness test indicated that the observed partial loudness was higher in all S/N ratios compared to the existing partial loudness model.

PACS Numbers: 43.50; 43.66

Keywords: wind turbine noise, natural ambient noise, masking

1. Introduction

In the light of global warming, an increased need of renewable power sources has led to an expansion of the wind power sectors in Europe. This development might accelerate further if the Kyoto protocol is signed by all industrialized countries. Although emissions of greenhouse gases from wind turbines are lower compared to the other power sources wind turbines are causing other disturbances to the nearby dwellings, for instance, emitting noise as well as interrupting the view. These malaises are accentuated in the regions often without industrial development where people generally have a higher sensitivity in deteriorating living conditions compared to the urban peoples who are used to living in noisy conditions and habituated to industrial landscapes. Natural ambient masking effects on wind turbine noise should therefore be evaluated in the process of optimization of wind energy output without causing disturbance to the nearby residents.

Among today's noise annoyance methods, the British [1] measures the background noise as A-weighed sound pressure level and thus correlates with the wind velocities to establish limits of noise emission from the wind turbines. The regulation is set to allow for wind turbine noise 5 dBA above background noise level. The German noise limit [2] is set to 45 dBA and the Dutch [3] uses wind speed dependent on the noise limits. Although some of these national standards consider the background noise level explicitly, to the authors' knowledge there have not been performed psychoacoustic tests to determine the signal to noise ratio for masking the wind turbines noise using different sources of ambient noises. A theoretical model on masking the wind turbine noise is available [4] but the validity of the model has not been tested by psychoacoustic experiment. Therefore, a laboratory study is performed and the results are compared with the existing partial loudness model [5, 6].

The objectives of the study are (i) to determine the threshold of wind turbine noise in the presence of natural ambient noise, (ii) to determine the S/N ratio between wind turbine and

natural noises, and (iii) to evaluate the partial loudness of wind turbine noise using existing partial loudness model. Two types of natural ambient noises are considered. One is the vegetation noise (i.e. noise from the trees) and the other one is the noise from sea waves. Two different test procedures are utilized to determine the threshold of wind turbine noise. The perceived proportion of wind turbine and natural ambient noises is examined using various S/N ratios. The partial loudness of wind turbine noise is tested by adjusting the loudness of a wind turbine noise with a partially masked wind turbine noise at different S/N ratios. Finally, the partial loudness of wind turbine noise was calculated using an existing partial loudness model [5, 6].

2. Theory of masking wind turbine noise

In this application the signal and the masker could be difficult to distinguish from each other, therefore, the signal (wind turbine noise) to noise (ambient noise) ratio for masking wind turbine noise is considered.

The loudness level [5, 6] is originated from the loudness model [7, 8]. The latter model is extended [5, 6] to better estimate partially masked sounds whose loudness levels are possible to estimate in a noisy background. This approach is thus utilized for evaluating the masking of wind turbines noise in the presence of background noise (natural ambient noise).

To compute the partial loudness model [5, 6] the third octave band spectrums are filtered into Equivalent Rectangular Bandwidth (*ERB*) bands and Excitation (*E*). The partial loudness, N'_{sig} in unit sones, is then calculated by summation across the N number of *ERB*s shown in Equation 1.

$$N'_{sig} = \sum_{n=1}^{N} \frac{c}{{E_0}^{\alpha}} [1 - \frac{kE_{n,noise}}{E_{n,sig}}] \cdot \left[({E_{n,sig}}^{\alpha} - {E_{thrq}}^{\alpha}) \right] \quad (1)$$

where c=0.0806, α=0.2106 are constants and k is the ratio of the signal power to noise power depending on frequency, E_0 the reference excitation produced by a 1 kHz sinusoid at 0 dB SPL (free field, frontal incidence), E_{nsig} and $E_{n,noise}$ are the excitations from the signal and noise at *ERB* number n. This model estimates the masking threshold when N'_{sig}=0.003. The excitation is transformed into excitation level, $L_{N,}$ in phon by Equation 2.

$$L_{N'_{sig}} = 40 + 10 \log_2 N'_{sig} \quad (2)$$

This model has been compared to the results of psychoacoustic tests [6]. However, the stimuli in the psychoacoustic test were artificial noises. These sounds could differ from the present study where recorded natural ambient noises and wind turbine sounds were used. Therefore, the validity of the existing model using the natural ambient noises as maskers and wind turbine noise as signal is also examined.

The combination of different noise sources were investigated in an earlier study [9]. The result of the study reveals that, as a rule of thumb, the dominating noise source is the one which is perceived as annoying. Therefore, the hypothesis is that the S/N ratio where the proportion of wind turbine noise is perceived as less than 50% of the total noise would determine the noise emission limit from the wind turbine without causing annoyance to the nearby residents [9].

3. Methods

3.1. Test sounds

The test sounds consisted of wind turbine noise and natural ambient noises. The natural ambient noises were mainly from sea wave noise and vegetation noises (see Figure 1). The vegetation noises were from coniferous and deciduous trees.

Coniferous and deciduous trees were chosen since they are very common in the vicinity of the residents where the wind turbines are installed. All the vegetation noises were recorded on a digital analyzer SONY PC216Ax using an omni-directional 1/2" microphone. The microphone

was placed 1.2 m above the ground level [10]. In order to decrease the pseudo-noise generated by the wind into the microphone a foam windscreen 10 cm in diameter was used to enclose the microphone. Both recordings were performed at times with high wind speeds, around 8 m/s, contributing to relatively high signal to noise ratios when vegetation noise levels are compared to the levels of other ambient noises.

The sea wave noise was recorded close to the shoreline. A low pass filter with a slope of 3 dB/octave band in higher frequency range (i.e. above 2.5 kHz) was applied in order to resemble with the perceived sea noise far from the shore. This was because buildings closer than 100 m from the sea shores are severely restricted in Sweden [11] and also because existing dwellings are not often located in the immediate vicinity of the shore.

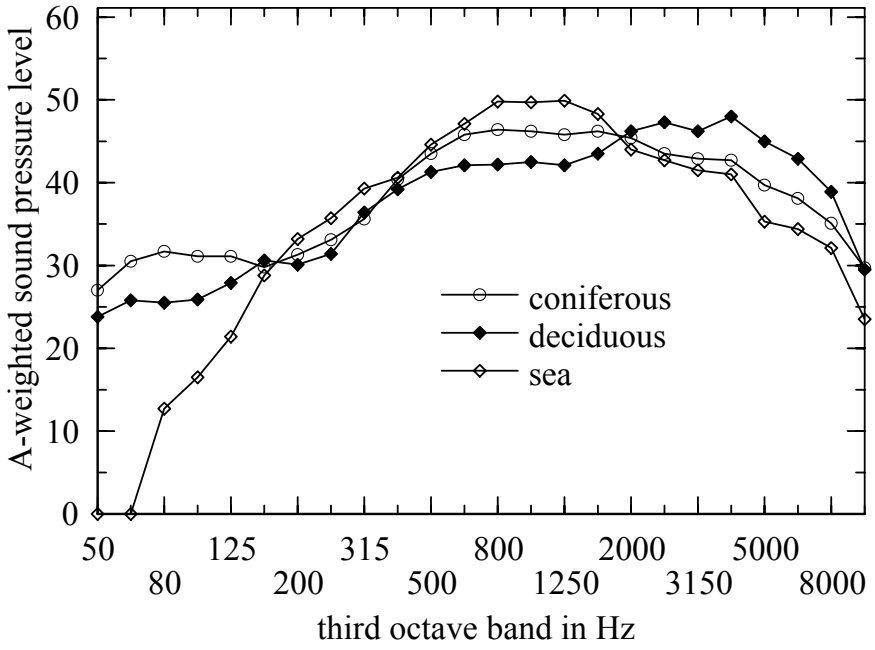

Figure 1: Third octave band spectra of natural ambient noises.

The wind turbine noise was recorded at a distance of 400 m from the Rhede wind turbines park at nighttime [12]. The microphone was mounted on a pole 4.5 m above the ground

level. The park consists of seventeen 1.8 MW wind turbines with a height of 98 m and 35 m blade radius.

All the natural ambient noise stimuli were normalized to a constant A-weighed sound pressure level of 56 dBA. This was due to the fact that the natural ambient noise is shown to be about this level. Each test signal was 3 s long with a fade in and fade out of 230 ms.

3.2. Subjects

Thirty six subjects participated in the study. They mainly consisted of staff and students from the Kungliga Tekniska Högskolan (KTH), Stockholm. Their ages varied between 15 and 52 years where. Nine subjects were females and 27 subjects were men.

3.3. Procedure

Four listening tests were assigned to each subject. All the listening tests were performed in a hemi-anechoic room where all monaurally recorded signals were presented through headphones AKG k-501 [9]. An audiometric test was administered to each subject prior to the listening test. All the subjects exhibited normal hearing abilities from 125 Hz to 8 kHz [14]. Two of the listening tests were to determine the threshold of wind turbine noise. The other two listening tests were to determine the S/N ratio and partial loudness.

3.3.1. Threshold tests

Two types of thresholds tests were administered to the subjects. The first threshold test was a discrimination test consisting of a criterion free four alternative four forced choice question (4A4FCQ) [15]. This means there were four noise samples. One noise sample contained both wind turbine noise and masking noise. The other three samples only contained the masking (natural ambient) noise. The subjects were instructed to determine which of the samples contained both wind turbine and masking noises from the four forced choice samples. The subjects had options to hear both wind turbine noise and ambient noise separately during the test.

If the subjects answered correctly, he/she was presented to lower S/N ratios and if incorrect new sound samples with higher S/N ratios were presented according to the flow chart in Figure 2. The figure shows the starting position of S/N=10 dBA at the top in the descending order and the flow followed depending on the responses of the subjects. In the ascending test the S/N ratios in Figure 2 are changing signs and also the arrows right and wrong are inversed.

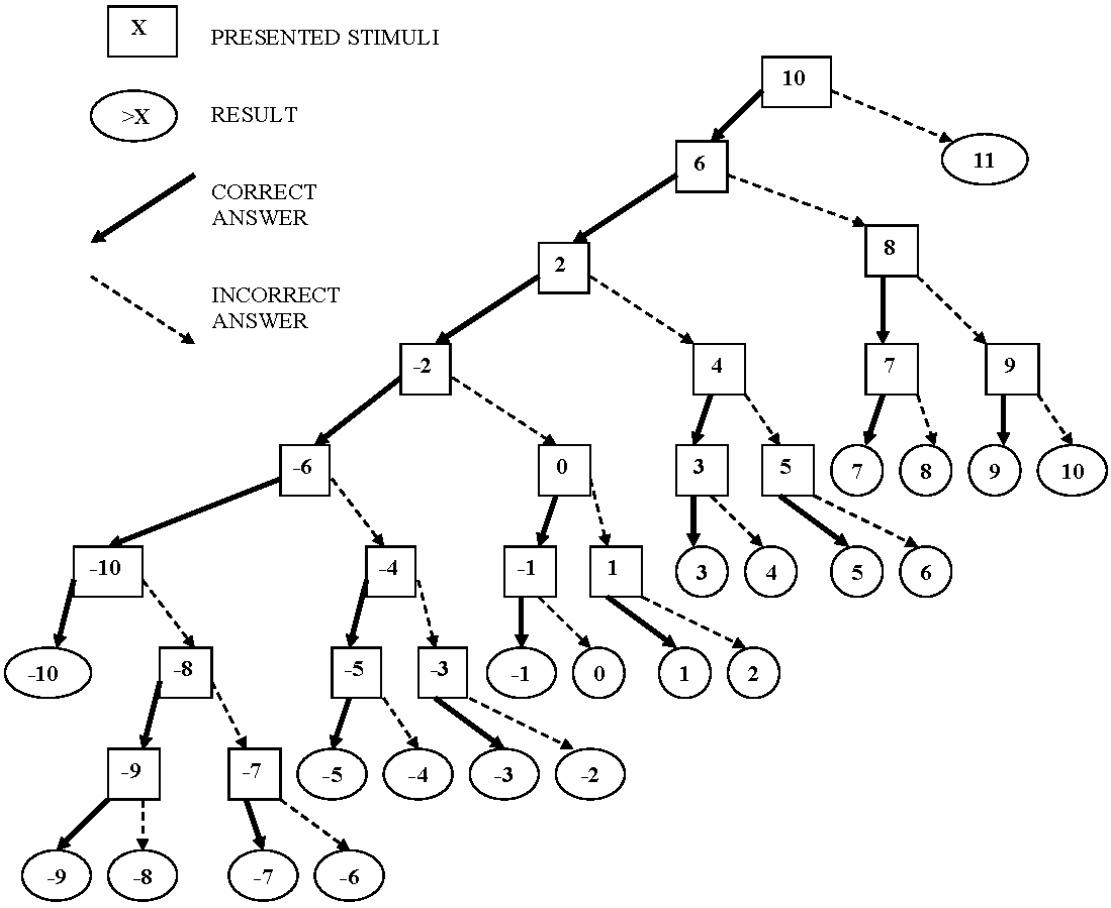

Figure 2: Flow chart of a four-forced choice threshold test in descending orders. The numbers show the S/N-ratio of wind turbine and a natural ambient noise.

Both ascending and descending orders were performed to reduce the biases from habituation and anticipation [15], the mean values from the ascending and descending task was defined as the masking threshold.

The second threshold test was designed to determine the just noticeable wind turbine noise from the natural ambient noise. A horizontal bar with a free marker was presented to the subjects. The position of the marker determines the hearing threshold of the wind turbine noise. The left end of the horizontal bar was allocated to the wind turbine noise whereas the right end of the horizontal bar was assigned to different S/N ratios of wind turbine and ambient noises. The subjects were instructed to drag the marker to the position where they perceived the wind turbine sound as just noticeable. The score of each judgment was recorded from the point of the marker which corresponded to a given S/N ratio. The test was repeated three times and the average value was considered as the masking threshold. To reduce the risk that subjects adjust the marker into the same position at every test, the random lengths of the ambient noise were placed on the horizontal bar and hence the same marker position yielded different S/N ratio.

The first threshold test was based on the forced choice S/N ratio whereas the second threshold test was based on the free choice S/N ratio. Two different threshold tests were chosen to examine the masking ability of natural ambient noise (first threshold test) as well as to determine the just noticeable wind turbine noise (second threshold test).

3.3.2. S/N ratio test

In this test, twelve stimuli, each with three seconds long, were randomly presented to the subjects. These stimuli consisted of different S/N-ratios (-3, 0, 3 or 6 dBA) of wind turbine and natural ambient noises (coniferous, deciduous and sea). The subjects had options to hear both wind turbine and ambient noises separately during the test. Subjects were asked to listen to the stimuli and judge the proportions of perceived wind turbine and natural ambient noises. The judgments were recorded on a linear scale ranging from 0 to 100% where “0” score on the scale means the proportion of wind turbine noise is not audible. On the other hand, score at “100%” on the scale indicates only the perception of wind turbine noise. For example, a judgment of 35 was

interpreted as the wind turbine noise constituting 35% of the perceived total sound whereas natural ambient noise constituted 65% of the presented stimulus.

3.3.3. Partial loudness test

To test the partial loudness, subjects listened to 12 pairs of stimuli. The first stimulus in the pair consisted of a wind turbine noise whereas the second stimulus in the pair consisted of different S/N ratios (0, 2, 4 or 6 dBA) between wind turbine noise and natural ambient noise. Each stimulus in the pair was presented for 3 s with a silent pause of 200 ms in between the pair. The signals duration were balanced between two contradictory objectives: long time, which enables the subjects to detect the wind turbine noise, and short time where the subjects should remember the loudness of the first signal. Subjects were asked to judge the equal loudness of the first stimulus (wind turbine noise) with the partial loudness of wind turbine noise in the second stimulus. A horizontal bar with a free marker was presented to the subjects to record the judgments of partial loudness. The bar was scaled from 1 to 100 where the position of the marker determines the loudness of the first stimulus (wind turbine noise) in phon [7]. The loudness of first stimulus (wind turbine noise) varied from 30 to 75 phon whereas the second stimulus (mixture of wind turbine & a natural ambient noise) had a constant total loudness of 60 phon, all loudness calculations were performed in the software MTS® Sound Quality version 3.7.

4. Results & Discussions

4.1. Judgments of thresholds

The analysis of variance in discrimination test shows that there are no significant differences in the first threshold test between the gender and natural ambient noises at 95% significance level. However, there is a significant difference in the threshold test between the natural ambient noises at 80% significance level, see Figure 3.

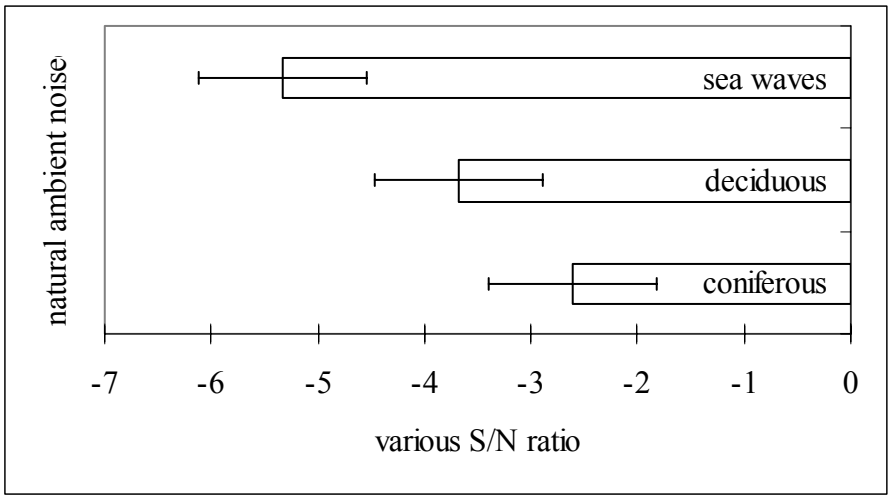

Figure 3. Error bar plot for the judgments of threshold in terms of S/N ratio in the discrimination test with means across listeners and a confidence interval of 95%.

Figure 3 shows that the S/N ratio is lower for the coniferous noise than the other ambient noises. This indicates that masking effect of coniferous trees is better than the other ambient noises.

The analysis of variance in the second threshold test shows that there is a significant difference in discriminating the wind turbine noise from the ambient noises in respect to various S/N ratios at a 95% significance level, see Figure 4. However, there is no significant difference shown between the genders in this threshold test.

Figure 4 shows that the S/N ratio is lower for the sea wave noise compared to the other ambient noises. This indicates that the masking effect of sea wave noise is lower than the other natural ambient noises. Here the masking effects of coniferous and deciduous noise are almost same.

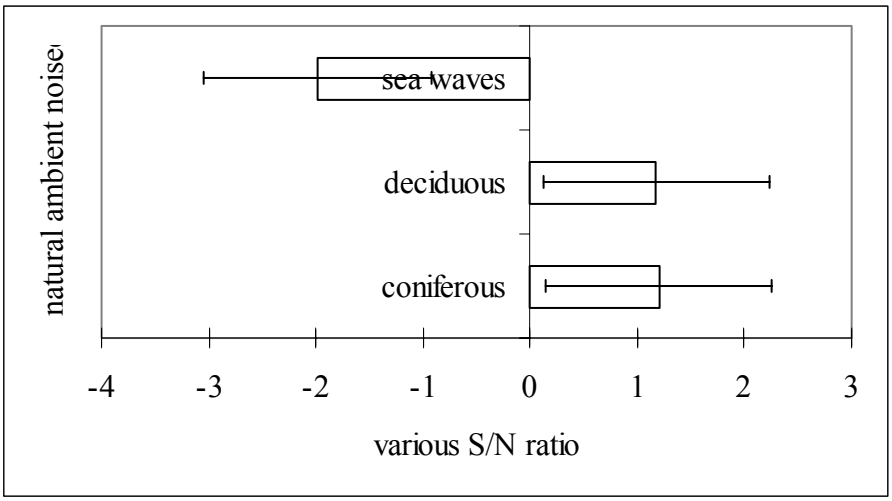

Figure 4. Error bar plot for the judgments of just noticeable wind turbine noise in terms of S/N ratio in the second threshold test with means and a confidence interval of 95%.

Both threshold tests indicate that the masking effect of sea noise is poorer than the other natural ambient noises. The first test indicates that the ability of masking wind turbine noise occur at S/N ratio of -3 dBA for ambient coniferous noise. On the other hand, the second threshold test shows that the wind turbine noise is noticeable at the S/N ratio of 1 dBA.

4.2. S/N ratio test

An analysis of variance conducted on the S/N ratio test results that there are significant differences in determining the wind turbine noise between the S/N ratios as well as between the natural ambient noises at a 95% significance level, see Figure 5. However, there is no significant difference between the genders in determining the wind turbine noise at a 95% significance level.

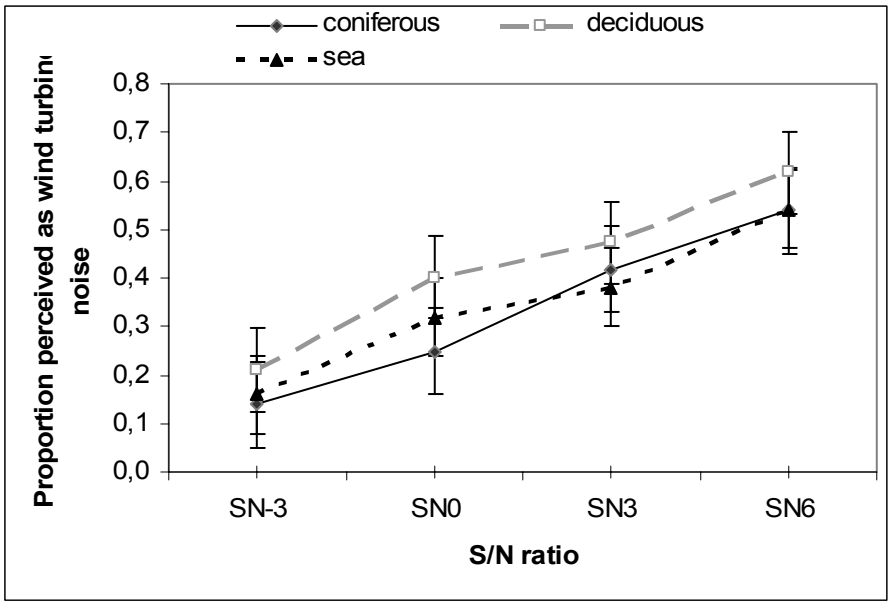

Figure 5. Error bar plot for the judgments of perceived proportion of wind turbine noise in respect to various S/N ratios with means and a confidence interval of 95%.

The Figure 5 shows that the perceived proportion of wind turbine noise is lower in the presence of coniferous noise than the other natural ambient noises and the perception of wind turbine noise is increased with the increase of S/N ratio. In this test, the perceived wind turbine noise in presence of sea noise is also shown lower compared to the deciduous noise. This might be due to the fact that A-weighted sound pressure level of coniferous and sea noises are higher in the frequency range of 500 – 2000 Hz (See Figure 1) which helps sea wave noise better to mask the wind turbine noise. The Figure also shows that the proportion of wind turbine noise is perceived as less than 50% of the total noise at S/N ratio of 3 dBA. Therefore, according to the hypothesis this level could be used as a limit to the noise emission of wind turbine which presumably would not disturb the residents. This ratio level is lower than the British standard of 5 dBA.

4.3. Partial loudness test

Analysis of variance in the partial loudness test shows that there are no significant differences between the natural ambient noises and S/N ratios as well as between the genders at a 95% significance level. However, there is a significant difference between the S/N ratios at a 90% significance level, see Figure 6.

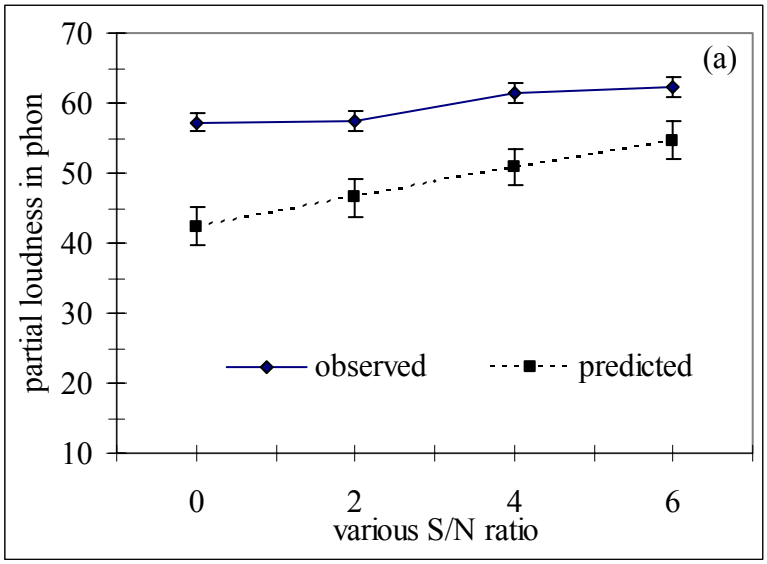

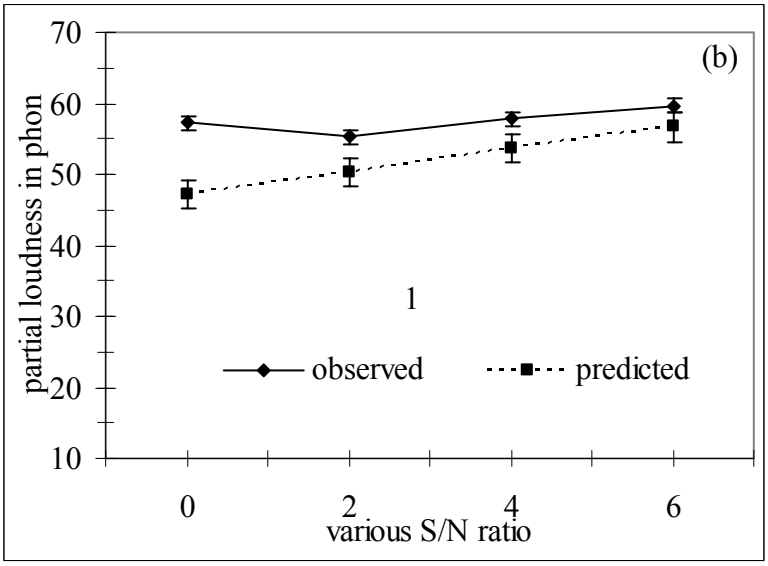

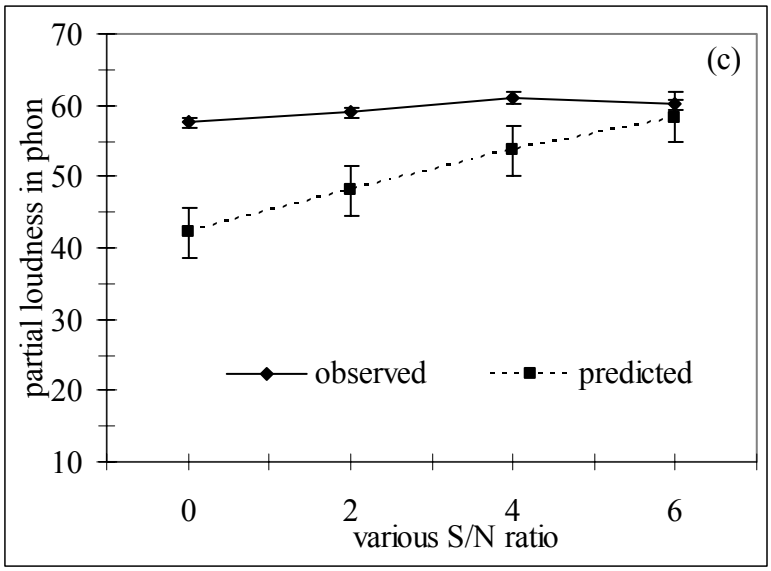

Figure 6. Error bar plot for the observed (according to the listening test) and predicted (according to Equation (2)) partial loudness in various S/N ratios for ambient noise of coniferous (a), deciduous (b) and sea wave (c) with means and a confidence interval of 95%.

The Figure 6 shows that the existing model underestimates the partial loudness of wind turbine noise in the presence of natural ambient noise at various S/N ratios. The partial loudness varies 10 – 15 dBA between observed and predicted values for the coniferous ambient noise. The observed partial loudness of wind turbine noise for all the ambient noises were almost equal for all S/N ratios. This might be due to the fact that the partial loudness of wind turbine noise is not easily separable from the total loudness which is assumed in the model [5]. On the other hand, the predicted (according to Equation 2) partial loudness increased with the increase of S/N ratio [5].

5. Conclusion

This study examined the potentiality of masking wind turbine noise using natural ambient noises. Thirty six subjects participated in four types of listening tests. The objectives of these tests were to determine the masked threshold, the proportion of perceived wind turbine noise in different

S/N ratios and finally compare the results of partial loudness (observed) with an existing theoretical model (predicted).

Both threshold tests as well as S/N ratio test revealed that the masking effects of coniferous noise was better for the wind turbine noise compared to the other natural ambient noises such as deciduous and sea noises. The results indicated that if the coniferous noise level is 2.5 dBA higher than the wind turbine noise, a complete masking will occur with a probability of 95%. On the other hand, sea wave noise level needs to increase 6.2 dBA above the wind turbine noise level to have the similar effect of masking. These S/N ratios could be used as a tool to construct noise emission guidelines for wind turbines in rural and recreational areas especially where natural ambient noise is only source of background noise.

Results from the partial loudness model [5, 6] and the judgments of loudness differed significantly. The existing partial loudness model underestimated the observed loudness by 10 – 15 phon at lower S/N ratios but these discrepancies decreased at higher S/N ratios.

It could be concluded that the S/N ratio of 3 dBA could be used as a limit to avoid annoyance which could be compared to the British guideline of 5 dBA higher for the background noise level. This result could be used as a tool for evaluating the potentiality of masking wind turbine noise using natural ambient noise in rural environments.

6. Acknowledgments

The authors would like to thank Swedish Energy Agency for their financial assistance. Thanks also remain to Prof. Mats Åbom for his support throughout the study. Marcus Wallenberg Laboratory for sound and vibration is also acknowledged for recording the ambient noises as well as conducting the listening tests.

7. References

[1] R. Meir & et al.: The assessment and rating of noise from wind farms. Technical report, ETSU-R-97, Department of Trade and Industry, 1996.

[2] TA -Lärm: Technische anleitungzum schutz gegen lärm (Technical Guideline for noise protection), Stand. GMBI. S. 503, **26** (August 1998) 1–20 (in German).

[3] A. W. Bezemer & et al.: Handleiding meten en rekenen industrielawaai (Manual for measuring and calculating industrial noise), (1999) 53–86 (in Dutch).

[4] O. Fégeant: On the masking of wind turbine noise by ambient noise. Proceedings of European Wind Energy, Nice, France (1999) 184–188.

[5] B. C. J. Moore, B. R. Glasberg and T. Baer: A Model for the prediction of thresholds, loudness and partial loudness. Journal of Audio Eng. Soc., **45** (1997) 224–240.

[6] B. C. J. Moore and B. R. Glasberg: A revision of Zwickers loudness model, Acta Acustica **82** (1996) 335–240.

[7] E. Zwicker: Über psykologische und metodische grundlagen der lautheit, Acustica **8** (1958) 237-258 (in German).

[8] E. Zwicker: Über die lautheit von ungedrosselten und gedrosselten schallen, Acustica **13** (1963) 194-211 (in German).

[9] B. Berglund, U. Berglund, M. Goldstein and T. Lindvall: Loudness (or annoyance) summation of combined community noise, Journal of Acoustical Society of America **70** (1981) 1628-1634.

[10] ISO1996: Acoustics – Description and measurement of environmental noise, International Organization for Standardization, Geneva, Switzerland (1986).

[11] Swedish Environmental Protection law, chapter 7 § 13-18.

[12] van den Berg G. P. Effects of the wind profile at night on wind turbine sound, Journal of Sound and Vibration **277** (2004) 955-970.

[13] van Wyk A. J.: A comparison of measurement methods for assigning human perception of loudness: An international survey, Acustica **49** (1981) 33-36.

[14] ISO 389: Acoustics – Standard reference zero for the calibration of pure-tone air conduction audiometers, International Organization for Standardization, Geneva, Switzerland (1991).

[15] S. A. Gelfand: Hearing, an introduction to psychological and physiological acoustics. Marcel Dekker, New York, 1998.